An approach for generating trajectory-based dynamics which conserves the canonical distribution in the phase space formulation of quantum mechanics. II. Thermal correlation functions

Jian Liu, and William H. Miller

Citation: J. Chem. Phys. **134**, 104102 (2011); doi: 10.1063/1.3555274
View online: https://doi.org/10.1063/1.3555274
View Table of Contents: http://aip.scitation.org/toc/jcp/134/10
Published by the American Institute of Physics

An approach for generating trajectory-based dynamics which conserves the canonical distribution in the phase space formulation of quantum mechanics. II. Thermal correlation functions

Jian Liu[a] and William H. Miller[b]
Department of Chemistry and K. S. Pitzer Center for Theoretical Chemistry, University of California, Berkeley, California 94720-1460, USA and Chemical Science Division, Lawrence Berkeley National Laboratory, Berkeley, California 94720-1460, USA

(Received 18 November 2010; accepted 19 January 2011; published online 8 March 2011)

We show the exact expression of the quantum mechanical time correlation function in the phase space formulation of quantum mechanics. The trajectory-based dynamics that conserves the quantum canonical distribution–equilibrium Liouville dynamics (ELD) proposed in Paper I is then used to approximately evaluate the exact expression. It gives exact thermal correlation functions (of even nonlinear operators, i.e., nonlinear functions of position or momentum operators) in the classical, high temperature, and harmonic limits. Various methods have been presented for the implementation of ELD. Numerical tests of the ELD approach in the Wigner or Husimi phase space have been made for a harmonic oscillator and two strongly anharmonic model problems, for each potential autocorrelation functions of both linear and nonlinear operators have been calculated. It suggests ELD can be a potentially useful approach for describing quantum effects for complex systems in condense phase. © *2011 American Institute of Physics*. [doi:10.1063/1.3555274]

I. INTRODUCTION

Thermal time correlation functions encode important dynamical information of complex systems.[1] For example, dipole moment correlation functions are related to infrared absorption spectra, flux correlation functions yield reaction rates, velocity correlation functions can be used to calculate diffusion constants, energy flux correlation functions produce thermal conductivities, and vibrational energy relaxation rate constants can be expressed in terms of force correlation functions. Thermal time autocorrelation functions are of the form

$$C_{AB}(t) \equiv \langle A(0)B(t)\rangle = \frac{1}{Z}\mathrm{Tr}(\hat{A}^{\beta} e^{i\hat{H}t/\hbar}\hat{B}e^{-i\hat{H}t/\hbar}), \tag{1}$$

where $\hat{A}^{\beta}_{\mathrm{std}} = e^{-\beta\hat{H}}\hat{A}$ for the standard version of the correlation function, or $\hat{A}^{\beta}_{\mathrm{sym}} = e^{-\beta\hat{H}/2}\hat{A}e^{-\beta\hat{H}/2}$ for the symmetrized version,[2] or $\hat{A}^{\beta}_{\mathrm{Kubo}} = \frac{1}{\beta}\int_0^{\beta} \mathrm{d}\lambda e^{-(\beta-\lambda)\hat{H}}\hat{A}e^{-\lambda\hat{H}}$ for the Kubo-transformed version.[3] These three versions are related to one another by the following identities between their Fourier transforms,

$$\frac{\beta\hbar\omega}{1-e^{-\beta\hbar\omega}} I^{\mathrm{Kubo}}_{AB}(\omega) = I^{\mathrm{std}}_{AB}(\omega) = e^{\beta\hbar\omega/2} I^{\mathrm{sym}}_{AB}(\omega), \tag{2}$$

where $I_{AB}(\omega) = \int_{-\infty}^{\infty} dt\, e^{-i\omega t} C_{AB}(t)$, etc. Here $Z = \mathrm{Tr}\,[e^{-\beta\hat{H}}]$ ($\beta = 1/k_B T$) is the partition function, $\hat{H}$ the (time-independent) Hamiltonian of the system with the total number of degrees of freedom N, which we assume to be of standard Cartesian form

$$\hat{H} = \tfrac{1}{2}\hat{\mathbf{p}}^T\mathbf{M}^{-1}\hat{\mathbf{p}} + V(\hat{\mathbf{x}}), \tag{3}$$

where $\mathbf{M}$ is the diagonal "mass matrix" with elements $\{m_j\}$, and $\hat{\mathbf{p}}$ and $\hat{\mathbf{x}}$ are the momentum and coordinate operators, respectively; and $\hat{A}$ and $\hat{B}$ are operators relevant to the specific property of interest.

There are two classes of practical trajectory-based methods for calculating these correlation functions for complex/large polyatomic molecular systems which achieve the exact quantum result as $t \to 0$ and approach the classical limit in the classical and high-temperature limits (i.e., $\hbar \to 0$ and $\beta \to 0$, respectively). One class of such approaches includes the so-called linearized SC-IVR (LSC–IVR) or classical Wigner model[4–10] and the forward–backward semiclassical dynamics (FBSD) approach,[11–27] which are based on various initial value representations (IVRs) of semiclassical (SC) theory.[28–44] The LSC–IVR/classical Wigner model gives the exact quantum correlation function in the short time limit[45] ($t \to 0$) and for harmonic potentials[6] (even for nonlinear operators, i.e., nonlinear functions of the position or momentum operators). The LSC–IVR has the drawback that the distribution generated for the operator $\hat{A}^{\beta}$ is not invariant with time for the case $\hat{A} = 1$ (i.e., $\hat{A}^{\beta} = e^{-\beta\hat{H}}$, the Boltzmann operator itself), which can be a serious problem if the long time behavior of the correlation function is important. The LSC–IVR/classical Wigner model also cannot describe true quantum coherence effects in time correlation functions, though it can describe quantum decoherence and tunneling effects very well.[5–8,22,46–58] The FBSD approach shares many properties of LSC–IVR.

Another class of approximate approaches that are comparable to LSC–IVR and FBSD include centroid molecular dynamics (CMD) (Refs. 59–61) and ring polymer molecular dynamics (RPMD).[62–64] Similar to LSC–IVR and FBSD, all these trajectory-based approaches fail to capture true quantum interferences but do describe quantum decoherence and tunneling effects fairly well and are relatively straightforward to

[a]Electronic mail: jianliu@berkeley.edu.
[b]Electronic mail: millerwh@berkeley.edu.

apply to complex polyatomic molecular systems for the entire range of temperature for systems of chemical interests. For both CMD and RPMD models, the quantum mechanical equilibrium distribution is conserved, i.e., for the case $\hat{A} = 1$, the correlation function is time independent. But both of these models fail to give the correct result if both operators [$\hat{A}$ and $\hat{B}$ in Eq. (1)] are nonlinear operators, even in a harmonic potential.[65,66] See Refs. 48, 49, 54, and 67 for more discussion and further comparisons. (Reference 67 shows that both CMD and RPMD models can cause serious problems in the high frequency regime even for correlation functions with linear operators.)

To summarize, LSC–IVR/FBSD and CMD/RPMD have different sets of properties, all of which are desirable. It would thus be appealing to have a trajectory-based dynamical method for thermal correlation functions which combines all these properties, i.e., which

1. conserves the quantum mechanical equilibrium distribution; and
2. produces the exact quantum correlation functions even for nonlinear functions of the position or momentum operators in the harmonic limit.

Such an approach was presented in our earlier work[6] using the Liouville equation for the Wigner distribution function, and this has been generalized in the preceding paper (Paper I) to various quantum phase space distribution functions.

The purpose of this paper is to show how these approaches, which we refer to as "equilibrium Liouville dynamics" (ELD), can be implemented in practice and to test them with various standard problems, to see how they perform compared to other approaches. Section II first shows the exact expression of the time correlation function in the phase space formulation of quantum mechanics, and Sec. III then discusses the "equilibrium distribution approximation" (EDA), which allows use of trajectory-based dynamics such as ELD for practical evaluation of the exact expression. Section IV and the Appendix present various approximations for the implementation of Wigner ELD (W-ELD) or Husimi ELD (H-ELD). Some numerical applications for the standard, Kubo-transformed, and symmetrized autocorrelation functions are demonstrated in Sec. V, including a harmonic model, a strongly anharmonic oscillator, and a more challenging quartic potential. Section VI summarizes and concludes.

II. THE EXACT FORMULATION OF THE CORRELATION FUNCTION IN THE PHASE SPACE FORMULATION OF QUANTUM MECHANICS

As a generalization of our recent work on improved versions of LSC–IVR,[6] it is straightforward to show, along similar lines to Paper I, that the time correlation function can be expressed in the phase space formulation of quantum mechanics in terms of a "general density operator" $\hat{A}^\beta(t) = e^{-i\hat{H}t/\hbar}\hat{A}^\beta e^{i\hat{H}t/\hbar}$ for systems at equilibrium, or more generally $\hat{A}^\beta(t) = e^{-i\hat{H}t/\hbar}\hat{\rho}_0\hat{A}e^{i\hat{H}t/\hbar}$ for any initial density $\hat{\rho}_0$ of the system. We give a brief summary below.

Quite a few representations[68–82] of the distribution function that have been proposed for the standard density operator $\hat{\rho}(t)$ (as discussed in Paper I) are also able to generate a *one-to-one* correspondence mapping from the general density operator $\hat{A}^\beta(t)$ to the phase space. In other words, replacing the standard density operator $\hat{\rho}(t)$ by the general density operator $\hat{A}^\beta(t)$ in Eq. (5) of Paper I, one obtains the expression of the correlation function in the phase space formulation of quantum mechanics

$$C_{AB}(t) = \frac{1}{Z}\int dx \int dp\ \mathsf{A}(x, p; t)\tilde{B}(x, p). \tag{4}$$

Here the "general" phase space distribution $\mathsf{A}(x, p; t)$ and the function $\tilde{B}(x, p)$ can be expressed in the unified classification scheme of Cohen[83] given by the following equations

$$\mathsf{A}(x, p; t) = \frac{1}{4\pi^2}\int d\zeta \times \int d\eta\ \mathrm{Tr}[\hat{A}^\beta(t)e^{i\zeta\hat{x}+i\eta\hat{p}}f(\zeta, \eta)]\ e^{-i\zeta x-i\eta p}, \tag{5}$$

$$\tilde{B}(x, p) = \frac{2\pi\hbar}{4\pi^2}\int d\zeta \times \int d\eta\ \mathrm{Tr}[f(-\zeta, -\eta)^{-1}e^{i\zeta\hat{x}+i\eta\hat{p}}\hat{B}]\ e^{-i\zeta x-i\eta p}. \tag{6}$$

For the general density operator $\hat{A}^\beta(t)$, the quantum Liouville theorem (von Neumann equation) describes how it evolves in time,

$$\frac{\partial\hat{A}^\beta(t)}{\partial t} = -\frac{1}{i\hbar}[\hat{A}^\beta(t), \hat{H}]. \tag{7}$$

By applying exactly the same procedure demonstrated in Appendix A of Paper I, one can show that Eq. (7) in the Wigner phase space representation becomes Eq. (36) of Paper I by replacing $\mathsf{P}_\mathrm{W}(x, p; t)$ by $\mathsf{A}_\mathrm{W}(x, p; t)$, and that in the Husimi phase space representation gives Eq. (37) of Paper I by replacing $\mathsf{P}_H(x, p; t)$ by $\mathsf{A}_H(x, p; t)$. Similarly, one can also express the phase space formulation of quantum Liouville's theorem for the general density operator $\hat{A}^\beta(t)$ with any of other distribution functions (and corresponding phase spaces) mentioned in Paper I.

In principle, if one could exactly solve the partial differential equations [i.e., Eq. (36) or (37) of Paper I by replacing $\mathsf{P}(x, p; t)$ by $\mathsf{A}(x, p; t)$], one would get the *exact dynamics* for the general phase space distribution $\mathsf{A}(x, p; t)$ and, thus, the exact quantum correlation function [Eq. (4)]. However, this task is intractable for large systems. We present another point of view in Sec. III, which allows one to solve the problem approximately.

III. EQUILIBRIUM DISTRIBUTION APPROXIMATION

A. Evaluation of the correlation function in classical mechanics

In classical mechanics, the phase space continuity equation or Liouville's theorem holds for the general density

distribution $\mathsf{A}_{cl}(x, p; t)$, i.e.,

$$\frac{\partial \mathsf{A}_{cl}(x, p; t)}{\partial t} = -\frac{\partial}{\partial x}\left(\mathsf{A}_{cl}\frac{p}{m}\right) + \frac{\partial}{\partial p}\left(\mathsf{A}_{cl}\frac{\partial V(x)}{\partial x}\right), \tag{8}$$

or

$$\frac{\partial \mathsf{A}_{cl}(x, p; t)}{\partial t} = -\frac{\partial}{\partial x}(\mathsf{A}_{cl}\dot{x}) - \frac{\partial}{\partial p}(\mathsf{A}_{cl}\dot{p}), \tag{9}$$

which states

$$\mathsf{A}_{cl}(x_t, p_t; t)dx_t dp_t = \mathsf{A}_{cl}(x_0, p_0; 0)dx_0 dp_0. \tag{10}$$

(It is easy to further show $\mathsf{A}_{cl}(x_t, p_t; t) = \mathsf{A}_{cl}(x_0, p_0; 0)$ along classical trajectory.)

The expression of the correlation function [i.e., Eq. (1) or Eq. (4)] in classical mechanics becomes

$$C_{AB}(t) = \frac{1}{Z_{cl}}\int dx \int dp \mathsf{A}_{cl}(x, p; t)B_{cl}(x, p). \tag{11}$$

Since the classical dynamics conserves the volume element of the phase space, Eq. (11) has the equivalent form

$$\begin{aligned} C_{AB}(t) &= \frac{1}{Z_{cl}}\int dx_t \int dp_t \mathsf{A}_{cl}(x_t, p_t; t)B_{cl}(x_t, p_t) \\ &= \frac{1}{Z_{cl}}\int dx_0 \int dp_0 \mathsf{A}_{cl}(x_0, p_0; 0)B_{cl}(x_t, p_t). \end{aligned} \tag{12}$$

In classical mechanics, the general density distribution is determined by its initial value along the trajectory

$$\mathsf{A}_{cl}(x_t, p_t; t) = \mathsf{A}_{cl}(x_0, p_0; 0) = \mathsf{P}^{eq}_{cl}(x_0, p_0; 0)A_{cl}(x_0, p_0), \tag{13}$$

which leads Eq. (12) to

$$\begin{aligned} C_{AB}(t) = \frac{1}{Z_{cl}}\int dx_0 \int dp_0 \mathsf{P}^{eq}_{cl}(x_0, p_0; 0) \\ \times A_{cl}(x_0, p_0)B_{cl}(x_t, p_t). \end{aligned} \tag{14}$$

Here A_{cl} and B_{cl} are the classical quantities corresponding to operators $\hat{A}$ and $\hat{B}$, respectively, and $Z_{cl} = \int dx_0 \int dp_0 \mathsf{P}^{eq}_{cl}(x_0, p_0; 0)$ is the classical partition function.

One sees that there are two ways for calculating the thermal correlation function in classical mechanics. One way is to solve the partial differential equation [Eq. (8)] in the Eulerian viewpoint, which is not feasible for large systems. The other is to evaluate the classical correlation function along classical trajectories, which conserve the classical canonical distribution, i.e.,

$$\frac{\partial \mathsf{P}^{eq}_{cl}(x, p; t)}{\partial t} = 0, \tag{15}$$

although the general density distribution $\mathsf{A}_{cl}(x, p; t)$ is in general not stationary, i.e.,

$$\frac{\partial \mathsf{A}_{cl}(x, p; t)}{\partial t} \neq 0. \tag{16}$$

The latter approach is conventional for calculating the correlation function in classical mechanics.

B. Evaluation of the correlation function with the trajectory-based dynamics in the phase space formulation of quantum mechanics

Making the analogy to the second approach for evaluating the correlation function in classical mechanics, we suppose that the thermal correlation function can be evaluated along the trajectories in dynamics that conserves the quantum canonical distribution, i.e.,

$$\frac{\partial \mathsf{P}^{eq}(x, p; t)}{\partial t} = 0, \tag{17}$$

such that

$$\begin{aligned} C_{AB}(t) = \frac{1}{Z}\int dx_0 \int dp_0 \mathsf{A}(x_0, p_0; 0) \\ \times \tilde{B}(x_t(x_0, p_0), p_t(x_0, p_0)). \end{aligned} \tag{18}$$

Although presented here in a new way, this is essentially the same as the "equilibrium distribution approximation" that we introduced in our earlier work.[6] It is easy to verify that Eq. (18) in principle gives the exact result at $t = 0$. The EDA allows the use of ELD, a family of trajectory-based dynamics satisfying Eq. (17), for evaluation of thermal correlation functions based on Eq. (18). As one can verify, for the case $\hat{A} = 1$, Eq. (18) reduces to the canonical ensemble average Eq. (51) in Paper I for $\langle B(t)\rangle$, which is time invariant for any trajectory-based dynamics satisfying Eq. (17).

For convenience, one can define the function f_{A^β}

$$f_{A^\beta}(x_0, p_0; 0) = \frac{\mathsf{A}(x_0, p_0; 0)}{\mathsf{P}^{eq}(x_0, p_0; 0)}, \tag{19}$$

as is often done in the Wigner phase space for the LSC–IVR.[6,47,48,54,55] For instance,

$$f^{\mathrm{W}}_{A^\beta}(x_0, p_0; 0) = \frac{\int d\Delta x \left\langle x - \frac{\Delta x}{2}\right| \hat{A}^\beta \left| x + \frac{\Delta x}{2}\right\rangle e^{ip\Delta x/\hbar}}{\int d\Delta x \left\langle x - \frac{\Delta x}{2}\right| e^{-\beta\hat{H}} \left| x + \frac{\Delta x}{2}\right\rangle e^{ip\Delta x/\hbar}}, \tag{20}$$

for the Wigner phase space, and

$$f^{H}_{A^\beta}(x_0, p_0; 0) = \frac{\langle x, p|\hat{A}^\beta|x, p\rangle}{\langle x, p|e^{-\beta\hat{H}}|x, p\rangle}, \tag{21}$$

for the Husimi phase space, and so on.

Then Eq. (18) for ELD becomes

$$\begin{aligned} C_{AB}(t) \equiv \langle A(0)B(t)\rangle = \frac{1}{Z}\int dx_0 \int dp_0 \mathsf{P}^{eq}(x_0, p_0; 0) \\ \times f_{A^\beta}(x_0, p_0; 0)\tilde{B}(x_t, p_t). \end{aligned} \tag{22}$$

Interestingly, one has

$$\begin{aligned} \langle A(t')B(t'+t)\rangle &= \frac{1}{Z}\int dx_0 \int dp_0 \mathsf{P}^{eq}(x_{t'}, p_{t'}; t') \\ &\quad \times f_{A^\beta}(x_{t'}, p_{t'}; t')\tilde{B}(x_{t'+t}, p_{t'+t}) \\ &= \frac{1}{Z}\int dx_0 \int dp_0 \mathsf{P}^{eq}(x_0, p_0; 0) \\ &\quad \times f_{A^\beta}(x_{t'}, p_{t'}; t')\tilde{B}(x_{t'+t}, p_{t'+t}), \end{aligned} \tag{23}$$

for ELD. One can prove that ELD gives the same results for Eq. (22) and for Eq. (23), by expressing the correlation function in a similar form to Eq. (D5) in Appendix D of Paper I.

Time-averaging Eq. (23) leads to

$$C_{AB}(t) = \frac{1}{T}\int_0^T dt' \langle A(t')B(t'+t)\rangle$$
$$= \frac{1}{Z}\int dx_0 \int dp_0\, \mathsf{P}^{eq}(x_0, p_0; 0)$$
$$\times \frac{1}{T}\int_0^T dt' f_{A^\beta}(x_{t'}, p_{t'}; t')\tilde{B}(x_{t'+t}, p_{t'+t}). \quad (24)$$

If the system is ergodic, Eq. (24) for ELD reduces to

$$C_{AB}(t) = \lim_{T\to\infty}\frac{1}{T}\int_0^T dt' f_{A^\beta}(x_{t'}, p_{t'}; t')\tilde{B}(x_{t'+t}, p_{t'+t}). \quad (25)$$

In Sec. IV, we arrive at explicit expressions for the correlation function within W-ELD and H-ELD.

IV. THERMAL GAUSSIAN APPROXIMATION (TGA) IN THE POSITION REPRESENTATION

Calculation of the function $\tilde{B}(x, p)$ for operator $\hat{B}$ [as defined in Eq. (6)] in Eqs. (22)–(25) is usually straightforward. In fact, $\hat{B}$ is often a function only of coordinates or only of momenta, in that case $\tilde{B}(x, p)$ in the Wigner phase space is simply the classical function itself. $\tilde{B}(x, p)$ in the Husimi phase space is the anti-Husimi function, which is

$$\tilde{B}_H(x, p) = x^2 - (2\Gamma)^{-1} \quad (26)$$

for $\hat{B} = \hat{x}^2$;

$$\tilde{B}_H(x, p) = p \quad (27)$$

for $\hat{B} = \hat{p}$, etc.

Calculating the Wigner or Husimi function $A(x, p)$ (or $f_{A^\beta}(x, p)$) for the operator $\hat{A}^\beta$, however, involves the Boltzmann operator with the total Hamiltonian of the complete system, so that carrying out the multidimensional Fourier transform to obtain it is far from trivial. Furthermore, it is necessary to do so in order to obtain the distribution of initial conditions of momenta p_0 and the ELD effective force [as defined in Eq. (46) in Paper I] of real-time trajectories. Here we use the Thermal Gaussian approximation (TGA) in the position representation, also known as the variational Gaussian wavepacket (VGW), which was first proposed by Hellsing *et al.*[84] and later modified by Mandelshtam *et al.*[85–87] to a more accurate version. We have implemented it into the LSC–IVR calculations recently.[6,22,47–49] In the VGW, the Boltzmann matrix element is approximated by a Gaussian form

$$\langle x|e^{-\tau\hat{H}}|q_0\rangle = \left(\frac{1}{2\pi}\right)^{N/2}\frac{1}{|\det(\mathrm{G}(\tau))|^{1/2}}\exp\left(-\frac{1}{2}(x-q(\tau))^T\mathrm{G}^{-1}(\tau)(x-q(\tau))+\gamma(\tau)\right), \quad (28)$$

$$\langle q_0|e^{-2\tau\hat{H}}|q_0\rangle = \int dx\, \langle q_0|\, e^{-\tau\hat{H}}\,|x\rangle\, \langle x|\, e^{-\tau\hat{H}}\,|q_0\rangle$$
$$= \left(\frac{1}{4\pi}\right)^{N/2}|\det(\mathrm{G}(\tau))|^{-1/2}\exp(2\gamma(\tau)), \quad (29)$$

where $\mathrm{G}(\tau)$ is an imaginary-time dependent real symmetric and positive-definite matrix, $q(\tau)$ the center of the Gaussian, and $\gamma(\tau)$ a real scalar function. The parameters are governed by the equations of motion:

$$\frac{d}{d\tau}\mathrm{G}(\tau) = -\mathrm{G}(\tau)\langle\nabla\nabla^T V(q(\tau))\rangle_{\mathrm{VGW}}\mathrm{G}(\tau) + \mathrm{h}^2 M^{-1},$$
$$\frac{d}{d\tau}q(\tau) = -\mathrm{G}(\tau)\langle\nabla V(q(\tau))\rangle_{\mathrm{VGW}},$$
$$\frac{d}{d\tau}\gamma(\tau) = -\frac{1}{4}\mathrm{Tr}(\langle\nabla\nabla^T V(q(\tau))\rangle_{\mathrm{VGW}}\mathrm{G}(\tau)) - \langle V(q(\tau))\rangle_{\mathrm{VGW}}. \quad (30)$$

with the notation

$$\langle h(q(\tau))\rangle_{\mathrm{VGW}} = \left(\frac{1}{\pi}\right)^{N/2}\frac{1}{|\det(\mathrm{G}(\tau))|^{1/2}}\int_{-\infty}^{\infty} dx \exp[-(x-q(\tau))^T\mathrm{G}^{-1}(\tau)(x-q(\tau))]h(x). \quad (31)$$

The initial conditions for the imaginary time propagation are

$$q(\tau \simeq 0) = q_0;\ G(\tau \simeq 0) = \hbar^2\tau M^{-1};$$
$$\gamma(\tau \simeq 0) = -\tau V(q_0). \quad (32)$$

The element of the Boltzmann operator can be expressed as

$$\langle x|\, e^{-\beta\hat{H}}\,|x'\rangle = \int dq_0\, \langle x|\, e^{-\beta\hat{H}/2}\,|q_0\rangle\, \langle q_0|\, e^{-\beta\hat{H}/2}\,|x'\rangle. \quad (33)$$

The expression for a partition function Z, for example, becomes

$$Z = \int dx \int dq_0 \langle x| e^{-\beta\hat{H}/2} |q_0\rangle \langle q_0| e^{-\beta\hat{H}/2} |x\rangle = \int dq_0 \frac{1}{(4\pi)^{N/2}} \frac{\exp\left(2\gamma\left(\frac{\beta}{2}; q_0\right)\right)}{\left|\det \mathrm{G}\left(\frac{\beta}{2}; q_0\right)\right|^{1/2}}. \quad (34)$$

A. W-ELD with full TGA

The Wigner density distribution can be written as

$$\mathrm{P}_{\mathrm{W}}^{eq,\,\mathrm{VGW}}(x, p) = \int dq_0 \rho_{\mathrm{W}}^{eq,\,\mathrm{VGW}}(x, p; q_0) \quad (35)$$

with

$$\rho_{\mathrm{W}}^{eq,\,\mathrm{VGW}}(x, p; q_0) = \frac{1}{(4\pi)^{N/2}} \frac{\exp\left(2\gamma\left(\frac{\beta}{2}; q_0\right)\right)}{\left|\det G\left(\frac{\beta}{2}; q_0\right)\right|^{1/2}} \cdot \frac{1}{\pi^{N/2}\left|\det \mathrm{G}\left(\frac{\beta}{2}; q_0\right)\right|^{1/2}} \exp\left(-\left(x - q\left(\frac{\beta}{2}; q_0\right)\right)^T \mathrm{G}^{-1}\left(\frac{\beta}{2}; q_0\right)\left(x - q\left(\frac{\beta}{2}; q_0\right)\right)\right) \cdot \frac{\left|\det \mathrm{G}\left(\frac{\beta}{2}; q_0\right)\right|^{1/2}}{\left(\pi\hbar^2\right)^{N/2}} \exp\left(-p^T \mathrm{G}\left(\frac{\beta}{2}; q_0\right) p/\hbar^2\right). \quad (36)$$

Because Eq. (35) requires an integral or a sum of imaginary trajectories for the calculation of the Wigner density distribution function, we refer to this method as "full TGA."

The function f_{A^β} [as defined in Eq. (19)] in the ELD formulation of the correlation function, i.e., Eqs. (22)–(25), can be evaluated together with full TGA. For instance,

$$\mathrm{Re}\left[f_{A^\beta}^{\mathrm{W}}(x, p)\right] = \frac{\int dq_0\, \rho_{\mathrm{W}}^{eq,\,\mathrm{VGW}}(x, p; q_0)\left[x^2 + \frac{G(\beta/2; q_0)}{2} - \frac{(G(\beta/2; q_0)\, p)^2}{\hbar^2}\right]}{\int dq_0\, \rho_{\mathrm{W}}^{eq,\,\mathrm{VGW}}(x, p; q_0)}, \quad (37)$$

for $\hat{A}^\beta = e^{-\beta\hat{H}}\hat{x}^2$;

$$f_{A^\beta}^{\mathrm{W}}(x, p) = \frac{\int dq_0\, \rho_{\mathrm{W}}^{eq,\,\mathrm{VGW}}(x, p; q_0)\left[\frac{2mG(\beta/2; q_0)p}{\beta\hbar^2}\right]}{\int dq_0\, \rho_{\mathrm{W}}^{eq,\,\mathrm{VGW}}(x, p; q_0)}, \quad (38)$$

for $\hat{A}^\beta = \hat{p}_{\mathrm{Kubo}}^\beta = \frac{i}{\hbar\beta} M[\hat{x}, e^{-\beta\hat{H}}]$; and

$$f_{A^\beta}^{\mathrm{W}}(x, p) = \frac{\int dq_0\, \rho_{\mathrm{W}}^{eq,\,\mathrm{VGW}}(x, p; q_0) f(q_0)}{\int dq_0\, \rho_{\mathrm{W}}^{eq,\,\mathrm{VGW}}(x, p; q_0)}, \quad (39)$$

for $\hat{A}^\beta = e^{-\beta\hat{H}/2} f(\hat{x}) e^{-\beta\hat{H}/2}$ where $f(x) = -\partial V(x)/\partial x$. It is straightforward to obtain Eqs. (37)–(39) from Eq. (20).

The full TGA gives the ELD effective force [as defined in Eq. (46) in Paper I] in the Wigner phase space as

$$-\frac{\partial}{\partial x} V_{\mathrm{eff}}^{\mathrm{W-ELD}}(x, p) = -\hbar^2 \left[\int dq_0 \rho_{\mathrm{W}}^{eq,\,\mathrm{VGW}}(x, p; q_0)\, \mathrm{G}\left(\frac{\beta}{2}; q_0\right)\right]^{-1} M^{-1} \times \left[\int dq_0 \rho_{\mathrm{W}}^{eq,\,\mathrm{VGW}}(x, p; q_0)\; \mathrm{G}\left(\frac{\beta}{2}; q_0\right)^{-1}\left(x - q\left(\frac{\beta}{2}; q_0\right)\right)\right]. \quad (40)$$

Implementing Eq. (40) in the equations of motion [Eq. (49) in Paper I], one is able to propagate ELD trajectories, from which the quantum thermal correlation function can be evaluated with Eqs. (22)–(25). W-ELD with full TGA has already been used in our earlier work.[6]

B. W-ELD with LGA–TGA

For the one-dimensional harmonic case $V(x) = 1/2\, M\omega^2 x^2$, note

$$G\left(\frac{\beta}{2};x\right)=\frac{\hbar}{M\omega}\tanh\left[\frac{\beta\hbar\omega}{2}\right], \tag{41}$$

$$\frac{\left\langle x-\frac{\Delta x}{2}\right|e^{-\beta\hat{H}}\left|x+\frac{\Delta x}{2}\right\rangle}{\langle x|\,e^{-\beta\hat{H}}\,|x\rangle}=\exp\left[-\frac{(\Delta x)^2}{4G\left(\frac{\beta}{2};x\right)}\right]. \tag{42}$$

As we have already mentioned the possibility in an earlier paper,[54] one can use the local Gaussian approximation (LGA) strategy[54] and Eq. (29) to obtain the Wigner density distribution function based on the VGW as

$$\begin{aligned}
&\mathsf{P}_W^{eq,\,\mathrm{LGA-TGA}}(x,p)\\
&=\frac{1}{(2\pi\hbar)^N}\langle x|\,e^{-\beta\hat{H}}\,|x\rangle\\
&\quad\times\int d\Delta x\frac{\langle x-\Delta x/2|\,e^{-\beta\hat{H}}\,|x+\Delta x/2\rangle}{\langle x|\,e^{-\beta\hat{H}}\,|x\rangle}e^{i\Delta x^T p/\hbar}\\
&=\langle x|\,e^{-\beta\hat{H}}\,|x\rangle\frac{\left|\det \mathrm{G}\left(\frac{\beta}{2};x\right)\right|^{1/2}}{(\pi\hbar^2)^{N/2}}\\
&\quad\times\exp\left[-p^T\mathrm{G}\left(\frac{\beta}{2};x\right)p/\hbar^2\right].\\
&=\frac{1}{(2\pi\hbar)^N}\exp\left[2\gamma\left(\frac{\beta}{2};x\right)\right]\\
&\quad\times\exp\left[-p^T\mathrm{G}\left(\frac{\beta}{2};x\right)p/\hbar^2\right]
\end{aligned} \tag{43}$$

We refer to this method as LGA–TGA.

By virtue of Eq. (46) in Paper I and Eq. (43), the LGA–TGA gives the ELD effective force as

$$\begin{aligned}
&-\frac{\partial}{\partial x}V_{\mathrm{eff}}^{\mathrm{W-ELD}}(x,p)\\
&\quad=\mathrm{G}\left(\frac{\beta}{2};x\right)^{-1}M^{-1}\\
&\quad\times\left[\hbar^2\frac{\partial\gamma\left(\frac{\beta}{2};x\right)}{\partial x}-\frac{1}{2}p^T\frac{\partial\mathrm{G}\left(\frac{\beta}{2};x\right)}{\partial x}p\right].
\end{aligned} \tag{44}$$

It is straightforward to show that the function f_{A^β} takes the form

$$\mathrm{Re}\left[f_{A^\beta}^{\mathrm{W}}(x,p)\right]=x^2+\frac{G\left(\frac{\beta}{2};x\right)}{2}-\frac{\left(G\left(\frac{\beta}{2};x\right)p\right)^2}{\hbar^2}, \tag{45}$$

for $\hat{A}^\beta=e^{-\beta\hat{H}}\hat{x}^2$;

$$f_{A^\beta}^{\mathrm{W}}(x,p)=\frac{2MG\left(\frac{\beta}{2};x\right)p}{\beta\hbar^2}, \tag{46}$$

for $\hat{A}^\beta=\hat{p}^\beta_{\mathrm{Kubo}}$;

$$f_{A^\beta}^{\mathrm{W}}(x,p)=-\left\langle\frac{\partial V\left(x'\left(\frac{\beta}{2};x\right)\right)}{\partial x'}\right\rangle_{\mathrm{VGW}} \tag{47}$$

for $\hat{A}^\beta=e^{-\beta\hat{H}/2}f(\hat{x})\,e^{-\beta\hat{H}/2}$, where the Gaussian average in Eq. (47) is given by Eq. (31).

LGA–TGA [Eqs. (43)–(47)] provides a more economic (but less accurate) way for calculating thermal correlation functions for multidimensional systems with W-ELD than full TGA [Eqs. (35)–(40)]. While full TGA involves storage of multiple imaginary-time trajectories so that the Wigner density distribution function at each phase space points (x,p) can be evaluated with those imaginary-time trajectories, LGA–TGA only requires propagating a single imaginary-time trajectory for each phase space point. We directly compare LGA–TGA and full TGA in our numerical examples in Sec. V.

C. H-ELD with full TGA

One can also obtain the Husimi density distribution based on the full TGA

$$\mathsf{P}_H^{eq,\,\mathrm{VGW}}(x,p)=\frac{1}{Z}\int dq_0\rho_H^{eq,\,\mathrm{VGW}}(x,p;\,q_0), \tag{48}$$

where

$$\begin{aligned}
\rho_H^{eq,\,\mathrm{VGW}}(x,p;\,q_0)=&\left(\frac{1}{2\pi}\right)^{\mathrm{N}/2}\frac{\exp\left(2\gamma\left(\frac{\beta}{2};\,q_0\right)\right)|\det\Gamma|^{1/2}}{\left|\det\left(1+\Gamma\mathrm{G}\left(\frac{\beta}{2};\,q_0\right)\right)\right|}\exp\left(-p^T\mathrm{G}\left(\frac{\beta}{2};\,q_0\right)\left(1+\Gamma\mathrm{G}\left(\frac{\beta}{2};\,q_0\right)\right)^{-1}p/\hbar^2\right)\\
&\times\exp\left(-\left(x-q\left(\frac{\beta}{2};\,q_0\right)\right)^{\mathrm{T}}\Gamma\left(1+\Gamma\mathrm{G}\left(\frac{\beta}{2};\,q_0\right)\right)^{-1}\left(x-q\left(\frac{\beta}{2};\,q_0\right)\right)\right).
\end{aligned} \tag{49}$$

Here Γ is the width parameter of the Husimi coherent state $|x,p\rangle$ [e.g., Eq. (10) or (22) of Paper I].
The ELD effective force in the Husimi phase space is

$$\begin{aligned}
-\frac{\partial}{\partial x}V_{\mathrm{eff}}^{\mathrm{H-ELD}}(x,p)=&-\hbar^2\left[\int dq_0\rho_H^{eq,\,\mathrm{VGW}}(x,p;\,q_0)\,\mathrm{G}\left(\frac{\beta}{2};\,q_0\right)\left(1+\Gamma\mathrm{G}\left(\frac{\beta}{2};\,q_0\right)\right)^{-1}\right]^{-1}M^{-1}\\
&\times\left[\int dq_0\rho_H^{eq,\,\mathrm{VGW}}(x,p;\,q_0)\;\Gamma\left(1+\Gamma\mathrm{G}\left(\frac{\beta}{2};\,q_0\right)\right)^{-1}\left(x-q\left(\frac{\beta}{2};\,q_0\right)\right)\right].
\end{aligned} \tag{50}$$

Note

$$\langle y|\, e^{-\beta\hat{H}/2}\hat{x}\,|x,\, p\rangle = \left(x - i\hbar\frac{\partial}{\partial p}\right)\langle y|\, e^{-\beta\hat{H}/2}\,|x,\, p\rangle\,, \tag{51}$$

$$\langle y|\, e^{-\beta\hat{H}/2}\hat{x}^2\,|x,\, p\rangle = \left(x - i\hbar\frac{\partial}{\partial p}\right)^2\langle y|\, e^{-\beta\hat{H}/2}\,|x,\, p\rangle\,. \tag{52}$$

It is easy to show

$$\begin{aligned}\mathrm{Re}\left[f^H_{A^\beta}(x,\, p)\right] = &\left[\int dq_0\; \rho_H^{eq,\,\mathrm{VGW}}(x,\, p;\; q_0)\right]^{-1}\int dq_0\; \rho_H^{eq,\,\mathrm{VGW}}(x,\, p;\; q_0)\\ &\times\left[\frac{G\left(\frac{\beta}{2};q_0\right)}{1+G\left(\frac{\beta}{2};q_0\right)\Gamma} - \frac{\left[G\left(\frac{\beta}{2};q_0\right)p\right]^2}{\hbar^2\left[1+G\left(\frac{\beta}{2};q_0\right)\Gamma\right]^2} + \frac{\left[q\left(\frac{\beta}{2};q_0\right)+G\left(\frac{\beta}{2};q_0\right)\Gamma x\right]^2}{\left[1+G\left(\frac{\beta}{2};q_0\right)\Gamma\right]^2}\right],\end{aligned} \tag{53}$$

for $\hat{A}^\beta = e^{-\beta\hat{H}}\hat{x}^2$;

$$\begin{aligned}f^H_{A^\beta}(x,\, p) = &\left[\int dq_0\; \rho_H^{eq,\,\mathrm{VGW}}(x,\, p;\; q_0)\right]^{-1}\\ &\times\int dq_0\; \rho_H^{eq,\,\mathrm{VGW}}(x,\, p;\; q_0)\\ &\times\left[\frac{2mG\left(\frac{\beta}{2};q_0\right)p}{\beta\hbar^2\left[1+G\left(\frac{\beta}{2};q_0\right)\Gamma\right]}\right],\end{aligned} \tag{54}$$

for $\hat{A}^\beta = \hat{p}^\beta_{\mathrm{Kubo}}$; and

$$f^H_{A^\beta}(x,\, p) = -\frac{\int dq_0\; \rho_H^{eq,\,\mathrm{VGW}}(x,\, p;\; q_0)\frac{\partial}{\partial q_0}V(q_0)}{\int dq_0\; \rho_H^{eq,\,\mathrm{VGW}}(x,\, p;\; q_0)}, \tag{55}$$

for $\hat{A}^\beta = e^{-\beta\hat{H}/2}f(\hat{x})\,e^{-\beta\hat{H}/2}$.

The relation

$$\langle\hat{A}(0)\ddot{\hat{A}}(0)\rangle = \left[\frac{d^2}{dt^2}\langle\hat{A}(0)\hat{A}(t)\rangle\right]_{t=0} = -\langle\dot{\hat{A}}(0)\dot{\hat{A}}(0)\rangle, \tag{56}$$

or around $\Gamma = M\omega/\hbar$ near the minimum of the potential well provides a good starting point for searching the optimum regime for the width parameter for H-ELD.

V. NUMERICAL EXAMPLES

A. Harmonic potential

It has already been demonstrated in Paper I and our earlier work[6] that W-ELD leads to classical dynamics for a harmonic potential (e.g., $V(x) = 1/2M\omega^2x^2$). More precisely, the W-ELD approach for the correlation function reduces to LSC–IVR in the harmonic limit. W-ELD therefore recovers exact quantum correlation functions of even nonlinear operators. Similarly, one can verify that this is also true for H-ELD when the width parameter is $\Gamma = M\omega/\hbar$.

Consider a harmonic potential $V(x) = 1/2M\omega^2x^2$ with $M = 1,\ \omega = 1$, and $\hbar = 1$. Figure 1 shows the correlation functions $\langle p(0)\,p(t)\rangle_{\mathrm{Kubo}}$ and $\left\langle x^2(0)\,x^2(t)\right\rangle_{\mathrm{std}}$ for a low temperature $\beta = 8$. Both W-ELD and H-ELD are able to produce the exact results as LSC–IVR does. In contrast, CMD and RPMD do not work well for correlation functions involving nonlinear operators even in the limit of a harmonic potential, as demonstrated in Fig. 1(d) and earlier by Horikoshi and Kinugawa in Fig. 1 of Ref. 66.

Although both ELD and LSC–IVR give exact correlation functions in the harmonic limit, ELD (W-ELD) can exhibit significant improvement over LSC–IVR for anharmonic potentials, as already discussed in our earlier work.[6] This is because ELD conserves the quantum canonical distribution, while LSC-IVR does not. ELD shares both the merits of LSC–IVR/FBSD and of CMD/RPMD. Here we focus on how well W-ELD and H-ELD perform within the framework of Eq. (18) [or Eq. (22), or (24)], comparing the results to the exact quantum correlation functions and the LSC–IVR values. (The classical correlation functions are not shown because they work poorly in low temperature region as demonstrated in the literature.[6,22]) We calculate the Kubo-transformed momentum autocorrelation function, the standard x^2 autocorrelation function, and the symmetrized force autocorrelation function (the latter two involving nonlinear local operators) for two one-dimensional anharmonic models.

B. Asymmetric anharmonic oscillator

The first anharmonic model is

$$V(x) = \tfrac{1}{2}M\omega^2x^2 - 0.10x^3 + 0.10x^4, \tag{57}$$

with $M = 1,\ \omega = \sqrt{2}$, and $\hbar = 1$. This quite anharmonic potential has been used as a benchmark system and discussed previously in the literature.[6,11,14,22,88,89] For full TGA described in Sec. IV, we use 21 imaginary trajectories for a high temperature $\beta = 0.1$ and 101 for a low temperature $\beta = 8$. These imaginary trajectories, once computed, are stored for use in the propagation of real-time ELD trajectories. For LGA–TGA, however, an imaginary trajectory has to be propagated at each real-time step of the ELD trajectory. The

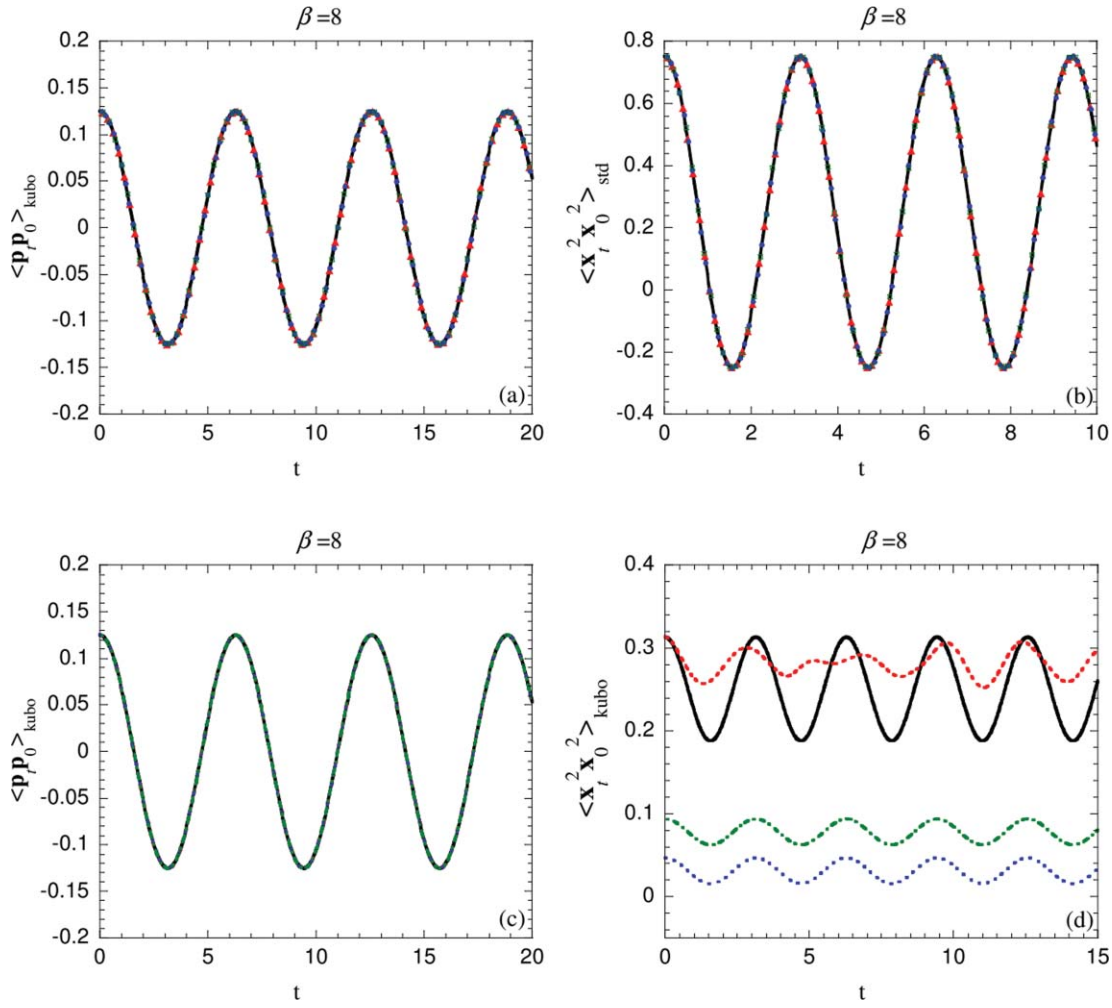

FIG. 1. The autocorrelation functions for the one-dimensional harmonic oscillator for $\beta = 8$. Panel (a) Kubo-transformed momentum autocorrelation function. (b) Real part of standard x^2 autocorrelation function. solid line: Exact quantum result; solid triangles: W-ELD; solid circles: H-ELD; hollow squares: LSC–IVR. Panel (c) Kubo-transformed momentum autocorrelation function. (d) Kubo-transformed x^2 autocorrelation function. Solid line: Exact quantum result; dashed line: RPMD; dotted line: CMD with classical operator; dot-dashed line: CMD with effective classical operator.

time-averaging technique [i.e., Eq. (24)] is used for the calculation of the correlation functions.

Consider W-ELD first. Results of the correlation functions are shown at a high temperature $\beta = 0.1$ in Fig. 2. Either W-ELD with full TGA or W-ELD with LGA–TGA gives correct results. This is not surprising since the ELD correlation functions approach the LSC–IVR results in the high temperature regime, where classical dynamics is a good approximation to the exact quantum correlation function. At a much lower temperature $\beta = 8$ (in Fig. 3), the correlation functions $\langle p(0)\, p(t)\rangle_{\text{Kubo}}$ and $\langle f(0)\, f(t)\rangle_{\text{mid}}$ calculated by W-ELD with full TGA match the exact quantum results almost perfectly, while $\left\langle x^2(0)\, x^2(t)\right\rangle_{\text{std}}$ by the same approach gives the amplitude of oscillation quite well but shows a slight frequency shift at long times. W-ELD with LGA–TGA performs similarly, though with slight dephasing in the amplitude. Both W-ELD with full TGA and W-ELD with LGA–TGA show systematical improvement over LSC–IVR at longer times.

Now consider H-ELD, focusing on the low temperature regime where quantum effects are important. The width parameter Γ of H-ELD is adjustable. As in other implementations of the Husimi coherent state in the literature,[39,90] there exists an optimum regime for the parameter, which depends on the frequency of the correlation function. [Equation (56) is a good starting point for searching the optimum regime.] For the present model, for example, these regimes are centered around $\Gamma = 1.52$ for $\langle p(0)\, p(t)\rangle_{\text{Kubo}}$ and $\langle f(0)\, f(t)\rangle_{\text{mid}}$, and about $\Gamma = 1.63$ for $\left\langle x^2(0)\, x^2(t)\right\rangle_{\text{std}}$. Figure 4 shows the correlation functions computed by H-ELD with full TGA with the optimum Γs. It is encouraging to note that the H-ELD correlation function with the optimum width parameter is a nearly perfect match to the exact quantum result.

C. Quartic potential

The next anharmonic model potential is

$$V(x) = \frac{x^4}{4}, \tag{58}$$

with $M = 1$ and $\hbar = 1$. Because no harmonic term is involved in the model, it represents a more challenging test since quantum rephrasing effects are much stronger. The simulation details for this potential are the same as those for the previous model.

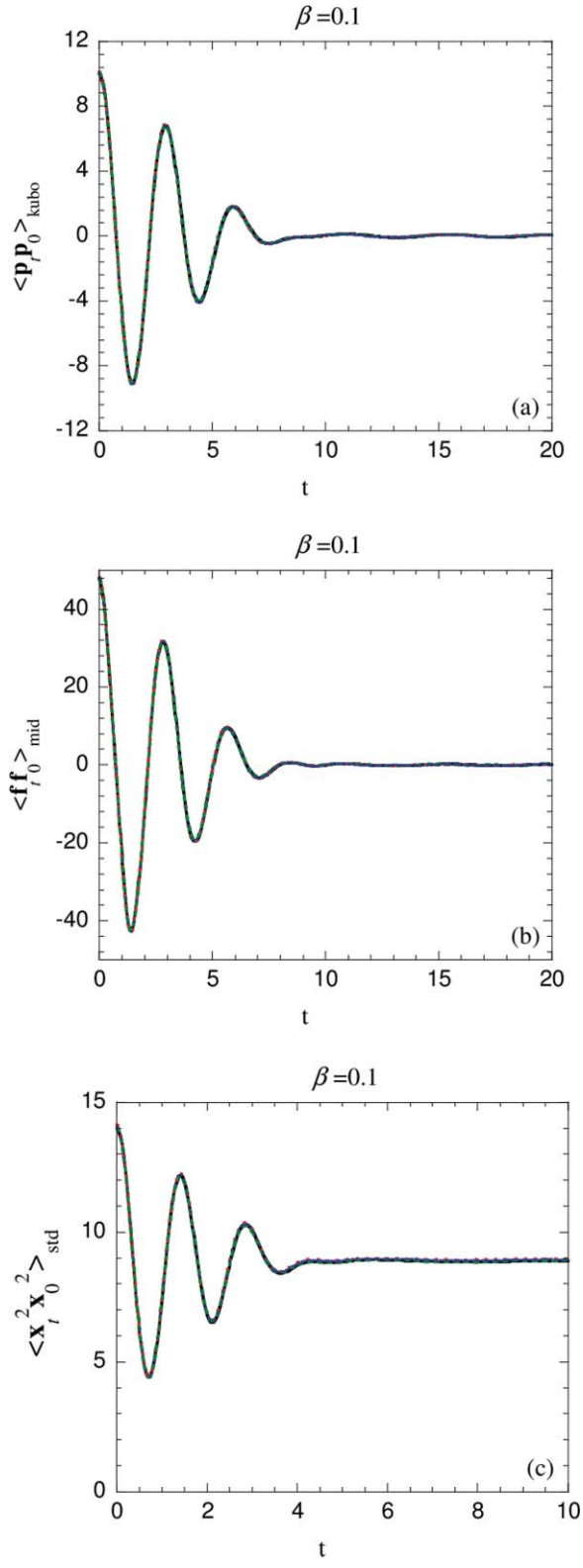

FIG. 2. The autocorrelation functions for the one-dimensional anharmonic oscillator for $\beta = 0.1$. Solid line: Exact quantum result. In the following results, the Boltzmann operator is treated by the TGA. Dotted line: W-ELD with full TGA. Solid circles: W-ELD with LGA–TGA. Dashed line: LSC–IVR with full TGA. Panel (a) Kubo-transformed momentum autocorrelation function. (b) Symmetrized force autocorrelation function. (c) Real part of standard x^2 autocorrelation function.

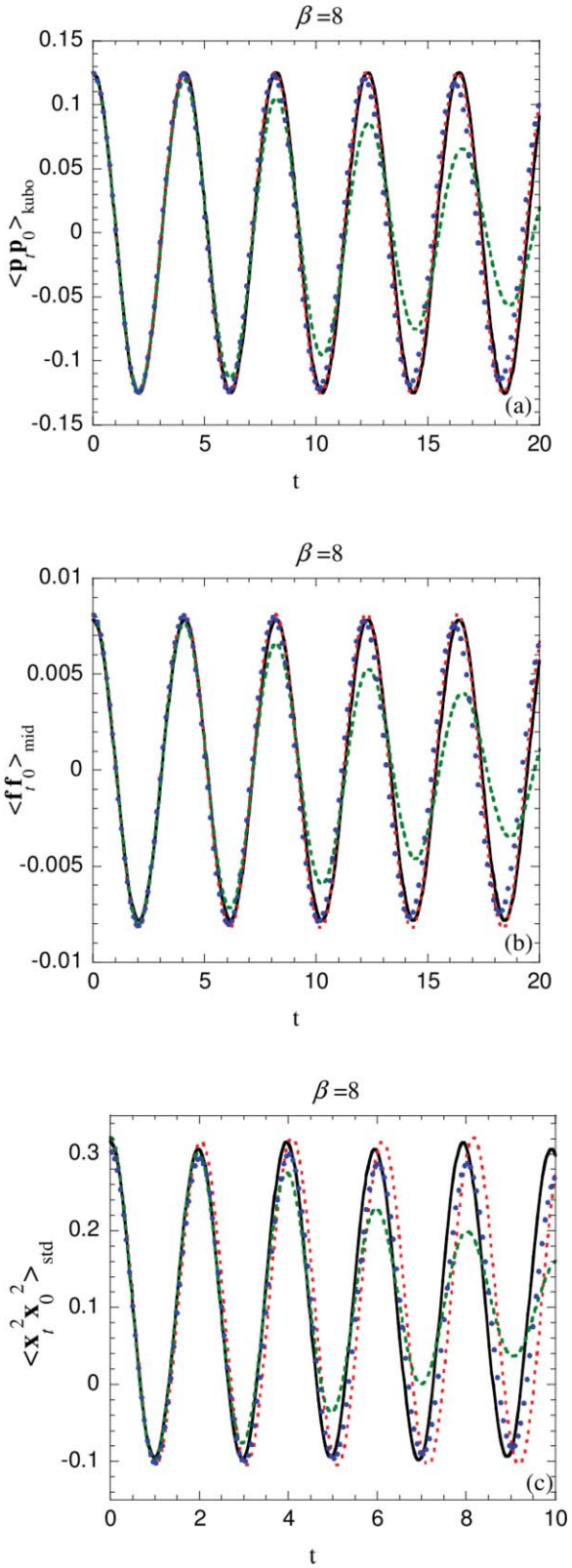

FIG. 3. As in Fig. 2, but for a much lower temperature $\beta = 8$.

Figure 5 shows that at the temperature $\beta = 0.1$ both W-ELD with full TGA and W-ELD with LGA–TGA can give correct results in the dephasing regime (up to three vibrational periods) but fails to describe the rephasing at longer times. (H-ELD behaves similarly, though the plot is not shown.) We

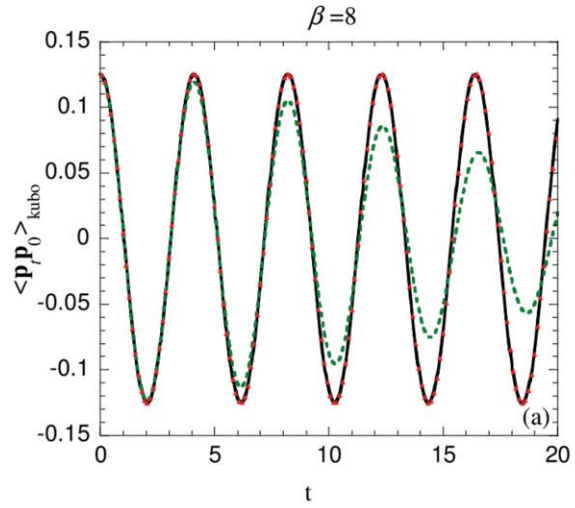

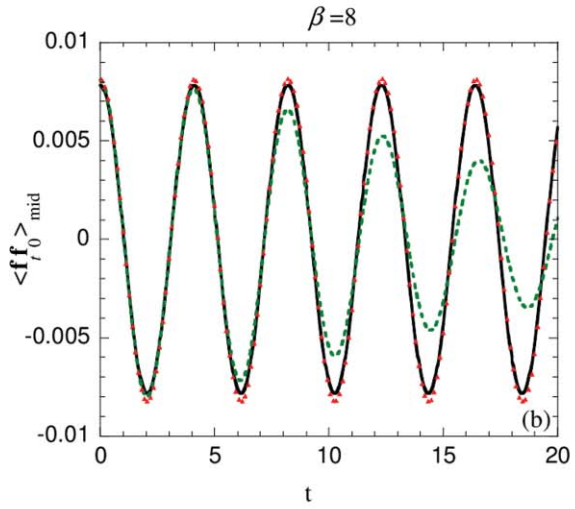

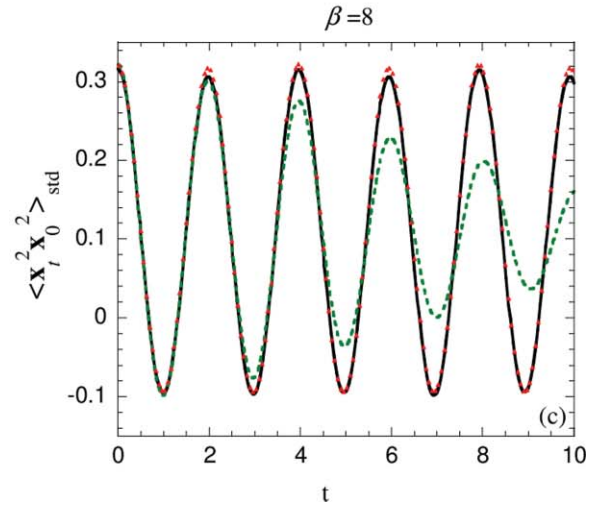

FIG. 4. The autocorrelation functions for the one-dimensional anharmonic oscillator for $\beta = 8$. Solid line: Exact quantum result. Solid triangles: H-ELD with full TGA. Dashed line: LSC–IVR with full TGA. Panel (a) Kubo-transformed momentum autocorrelation function. (b) Symmetrized force autocorrelation function. (c) Real part of standard x^2 autocorrelation function.

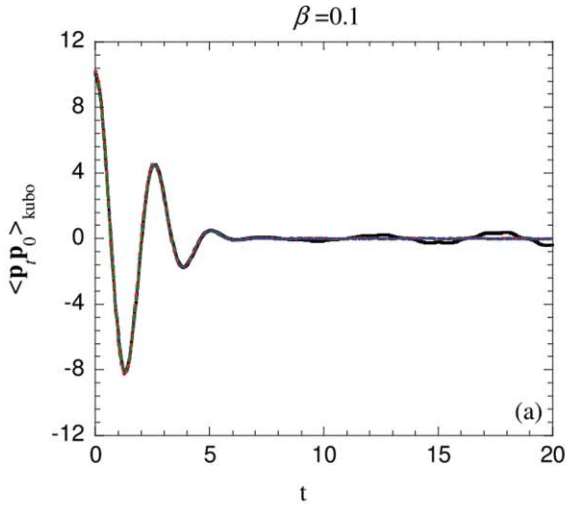

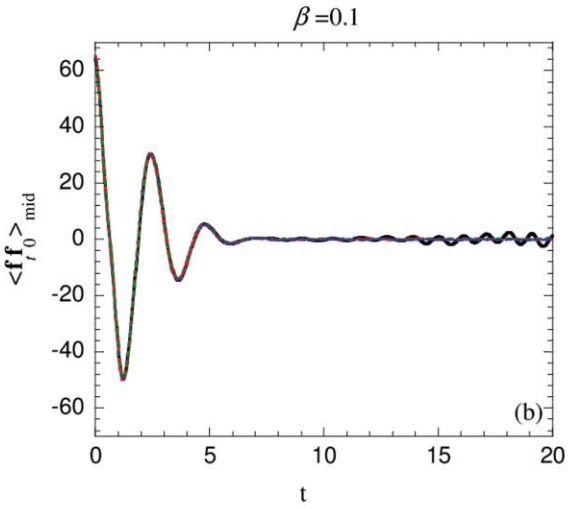

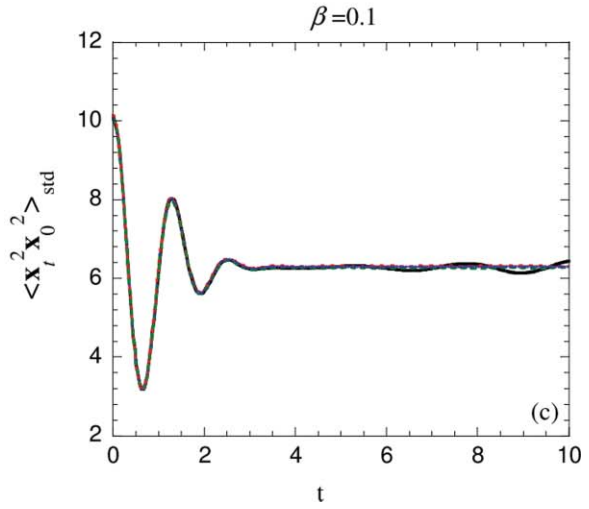

FIG. 5. The autocorrelation functions for the one-dimensional quartic oscillator for $\beta = 0.1$. Solid line: Exact quantum result. In the following results, the Boltzmann operator is treated by the TGA. Dotted line: W-ELD with full TGA. Solid circles: W-ELD with LGA–TGA. Dashed line: LSC–IVR with full TGA. Panel (a) Kubo-transformed momentum autocorrelation function. (b) Symmetrized force autocorrelation function. (c) Real part of standard x^2 autocorrelation function.

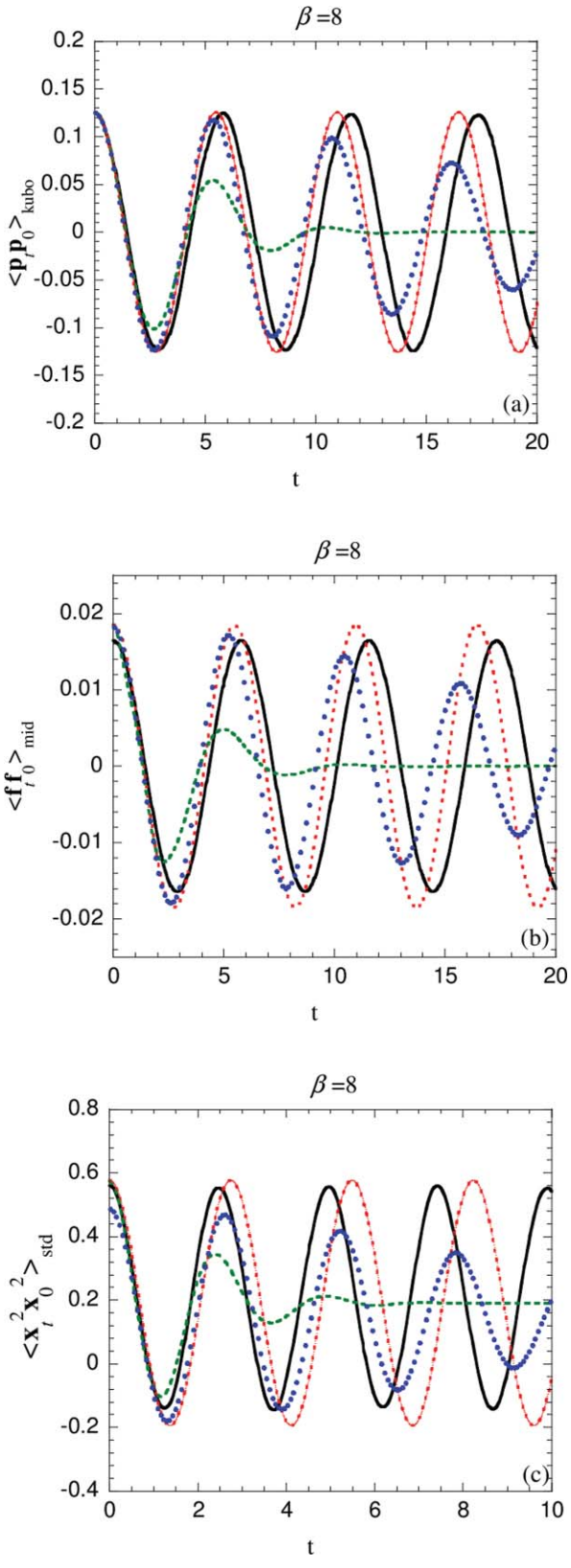

FIG. 6. As in Fig. 5, but for a much lower temperature $\beta = 8$.

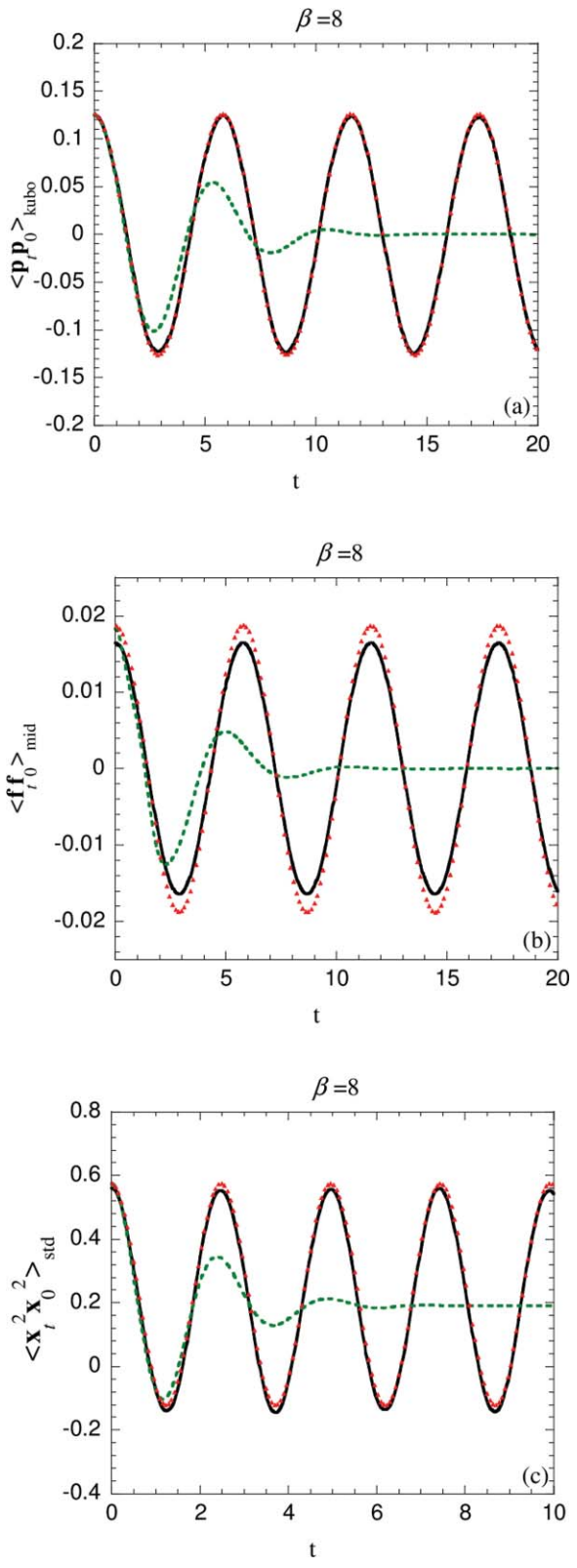

FIG. 7. The autocorrelation functions for the one-dimensional quartic oscillator for $\beta = 8$. Solid line: Exact quantum result. Solid triangles: H-ELD with full TGA. Dashed line: LSC–IVR with full TGA. Panel (a) Kubo-transformed momentum autocorrelation function. (b) Symmetrized force autocorrelation function. (c) Real part of standard x^2 autocorrelation function.

may infer that the EDA (introduced in Sec. III) is incapable of describing long-time quantum coherence effects. (For example, the EDA is not good for describing quantum coherence or interference effects in a one-dimensional double-well system.) However, one would often expect such long-time

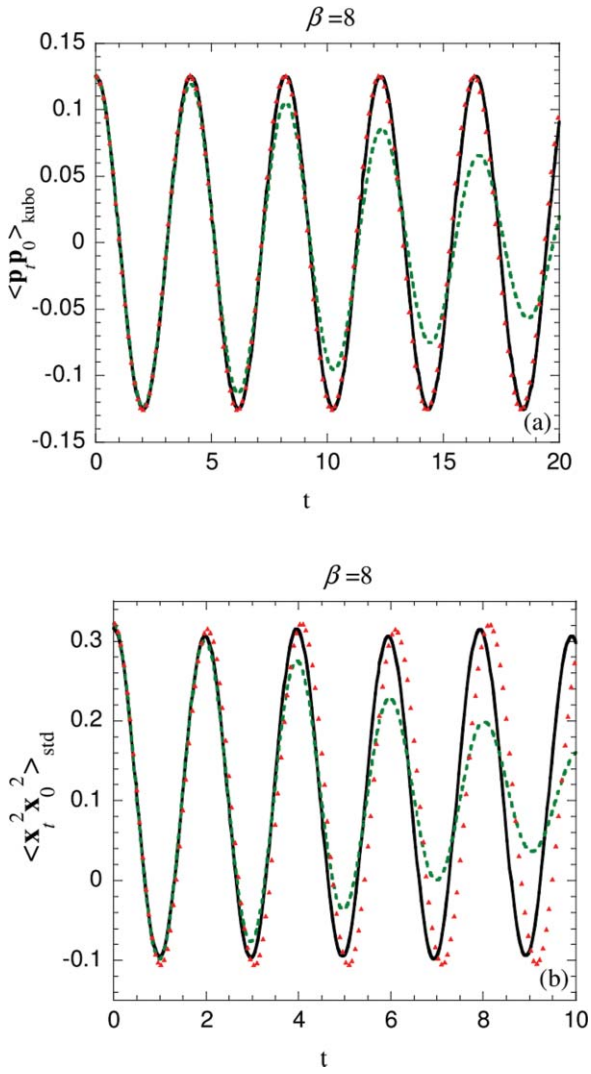

FIG. 8. The autocorrelation functions for the one-dimensional anharmonic oscillator for $\beta = 8$. Solid line: Exact quantum result. Solid triangles: W-ELD with FKA. Dashed line: LSC–IVR with full TGA. Panel (a) Kubo-transformed momentum autocorrelation function. (b) Real part of standard x^2 autocorrelation function.

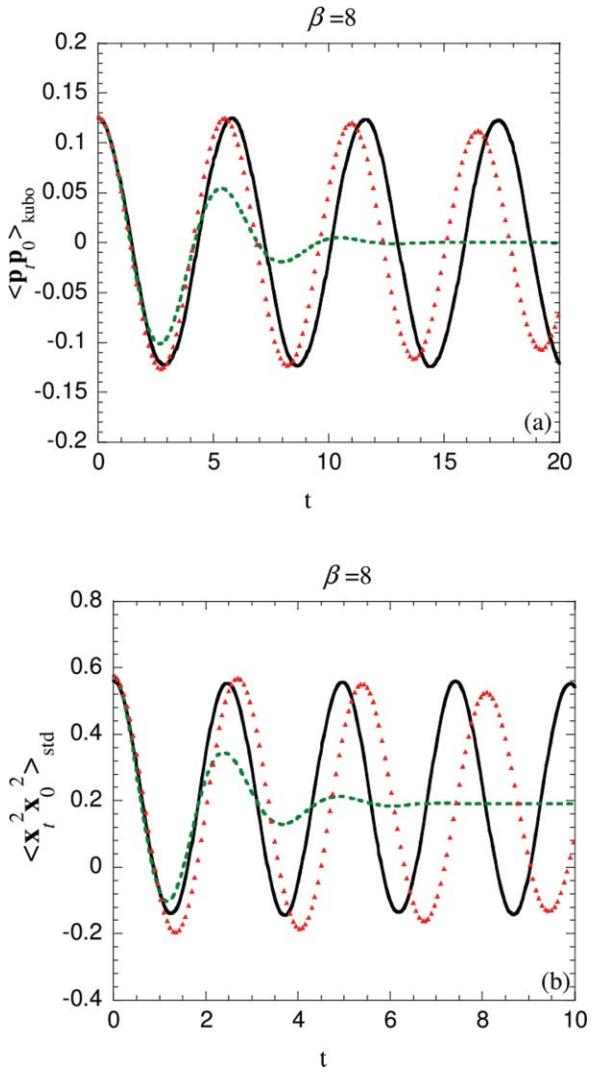

FIG. 9. The autocorrelation functions for the one-dimensional quartic oscillator for $\beta = 8$. Solid line: Exact quantum result. Solid triangles: W-ELD with FKA. Dashed line: LSC–IVR with full TGA. Panel (a) Kubo-transformed momentum autocorrelation function. (b) Real part of standard x^2 autocorrelation function.

rephrasing effects to be quenched by coupling among the various degrees of freedom in condensed phase systems;[42,91,92] the most important behavior to capture in these cases is the short-time dephasing in the correlation function, for which ELD can provide an accurate description.

Results for the much lower temperature ($\beta = 8$) are shown in Figs. 6 (for W-ELD) and 7 (for H-ELD). W-ELD with full TGA describes the amplitude of oscillation quite well (the small residual error originating in the TGA treatment) with a noticeable frequency shift after one vibrational period. W-ELD with LGA–TGA behaves similarly with more dephasing in the amplitude. With optimum coherent state width parameters, H-ELD with full TGA can almost reproduce the exact quantum correlation functions. For the present model, the optimum widths lie around $\Gamma = 1.03$ for $\langle p(0)p(t)\rangle_{\text{Kubo}}$ and $\langle f(0)f(t)\rangle_{\text{mid}}$, and around $\Gamma = 1.40$ for $\langle x^2(0)x^2(t)\rangle_{\text{std}}$ for the quartic model. Any of these ELD methods significantly improve over LSC–IVR, which dephases too quickly after the first vibrational period.

VI. CONCLUSIONS

In this paper we have shown that the exact time correlation function [Eq. (1)] can be expressed in the form of Eq. (4) in the phase space formulation of quantum mechanics. For thermal equilibrium systems, the EDA invites trajectory-based dynamics that conserves the canonical distribution in the phase space formulation of quantum mechanics, which provides a practical and reasonably good approximation for calculating the thermal correlation function [Eq. (18)]. The ELD introduced in Paper I is such a family of trajectory-based dynamics. It is able to give exact correlation functions (of even nonlinear operators) in the classical, high temperature, and harmonic limits.

Both Wigner and Husimi distribution functions have been used for applications of the ELD correlation function in the paper. (One can of course use other distribution functions to implement ELD.) Both W-ELD and H-ELD capture appreciable quantum effects in the correlation functions for

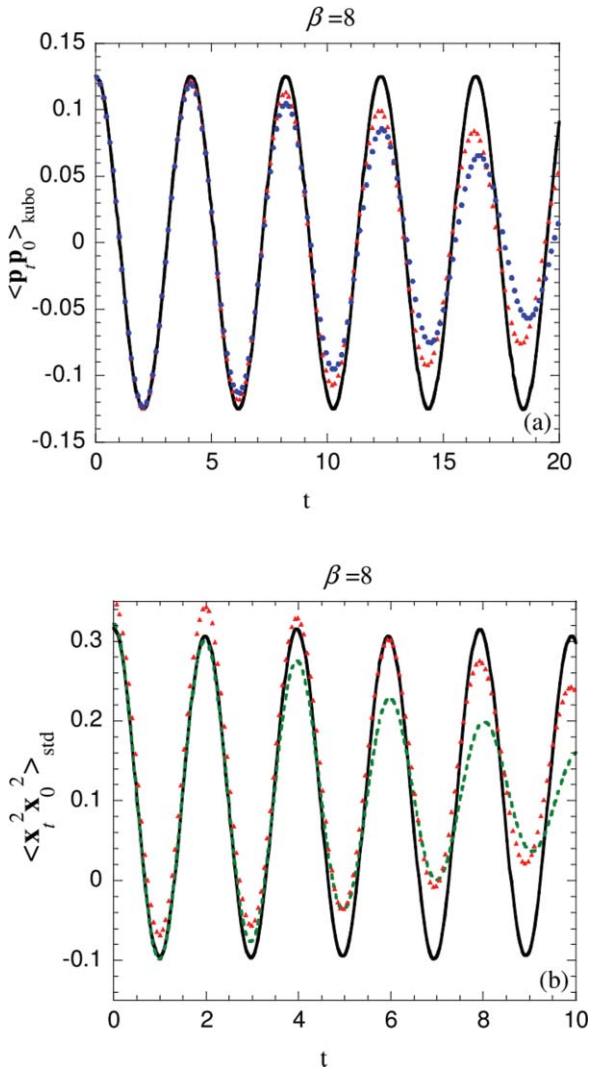

FIG. 10. The autocorrelation functions for the one-dimensional anharmonic oscillator for $\beta = 8$. Solid line: Exact quantum result. Solid triangles: H-ELD with TFG. Dashed line: LSC–IVR with full TGA. Panel (a) Kubo-transformed momentum autocorrelation function. (b) Real part of standard x^2 autocorrelation function.

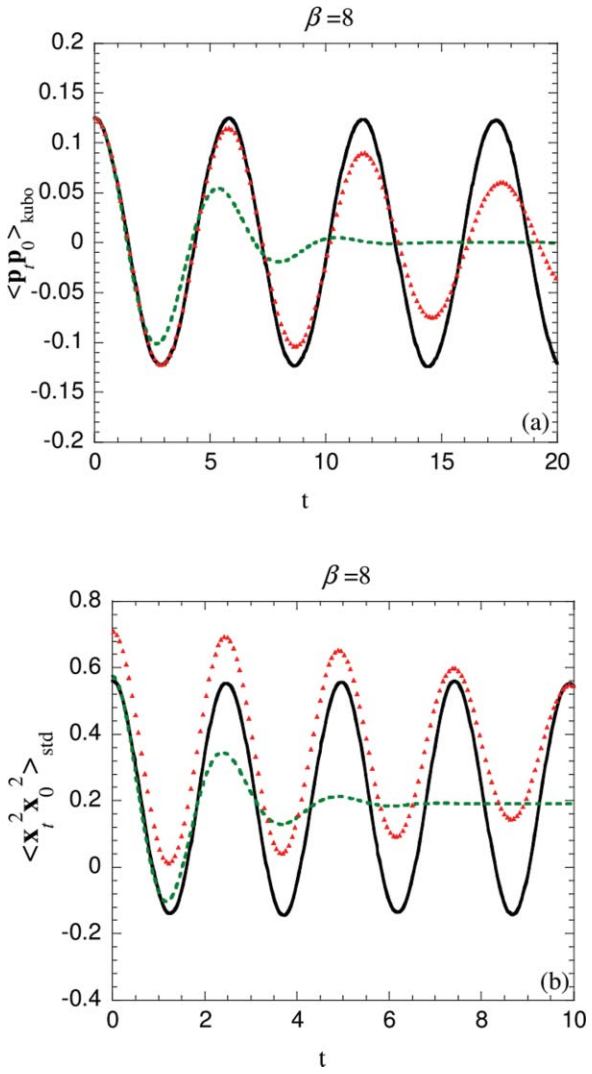

FIG. 11. The autocorrelation functions for the one-dimensional quartic oscillator for $\beta = 8$. Solid line: Exact quantum result. Solid triangles: H-ELD with TFG. Dashed line: LSC–IVR with full TGA. Panel (a) Kubo-transformed momentum autocorrelation function. (b) Real part of standard x^2 autocorrelation function.

short times, for all temperatures. In low temperature regime, W-ELD is more convenient to implement and can give reasonably good results, while H-ELD is capable of producing nearly exact quantum correlation functions when the width parameter chosen is optimized. A subject for future study is how one can develop criteria for efficiently locating the optimum regime in the width parameter space for the H-ELD correlation function (for large systems). A possible way is to start from Eq. (56) or around $\Gamma = M\omega/\hbar$ near the minimum of the potential well, and then to use the H-ELD result as *a priori* for maximum entropy analytic continuation (MEAC). As suggested in our earlier work,[49] the MEAC correction should be applicable to any approximate method for describing quantum dynamics. If the MEAC procedure does little correction to the H-ELD result, it is likely that the width parameter is optimum.

Combined with the TGA in the position representation (discussed in Sec. IV) or other local harmonic/Gaussian approximations (introduced in the Appendix) for the Boltzmann operator, W-ELD and H-ELD offer feasible tools for calculating thermal correlation functions for complex systems in the condensed phase, because they do not involve oscillatory factors in the necessary phase space averages [see Eqs. (22)–(25)]. The W-ELD with LGA–TGA (or H-ELD with thermal frozen Gaussian (TFG) or thermal thawed Gaussian (TTG) as discussed in the Appendix) offers a more practical and promising method for large systems. (An efficient path integral representation of ELD will be discussed in a subsequent paper.) The MEAC+ELD approach is also auspicious because ELD offers an even better prior than LSC–IVR (and other comparable methods). Further work along these lines for realistic polyatomic molecular systems in condensed phase would certainly be of interest.

ACKNOWLEDGMENTS

J.L. thanks Dr. Shervin Fatehi for reading the manuscript and giving useful comments. This work was supported by

the National Science Foundation Grant No. CHE-0809073 and by the Director, Office of Science, Office of Basic Energy Sciences, Chemical Sciences, Geosciences, and Biosciences Division, U.S. Department of Energy under Contract No. DE-AC02–05CH11231. We also acknowledge a generous allocation of supercomputing time from the National Energy Research Scientific Computing Center (NERSC) and the use of the Lawrencium computational cluster resource provided by the IT Division at the Lawrence Berkeley National Laboratory.

APPENDIX: MORE APPROACHES FOR ELD

One sees from Sec. IV that the central task in implementing ELD is to evaluate the phase space distribution function (e.g., Wigner or Husimi function) for the Boltzmann operator. Besides the TGA in the position representation introduced in Sec. IV, several other approximations have already been introduced in order to get the Wigner function of the Boltzmann operator in the literature, which include the harmonic approximation by Wang *et al.*,[4] the *local* harmonic approximation by Shi and Geva,[8] the Feynman–Kleinert approximation by Poulsen *et al.*,[7] and the local Gaussian approximation by Liu and Miller which improves on all these approximations for treating imaginary frequencies.[54] Most of these approximations are also useful to obtain the Husimi function of the Boltzmann operator. The pair-product approximation[93] introduced to FBSD by Nakayama and Makri[15] is also useful to obtain the Husimi or Wigner density distribution function in ELD. In the following, we show how ELD can be implemented with the FKA or other two TGAs in the coherent state representation.

1. Feynman–Kleinert approximation (FKA)

The FKA (Refs. 94 and 95) has been used by Cuccoli *et al.*[96] to calculate the Wigner density distribution for the Boltzmann operator and later introduced by Poulsen *et al.* in the LSC–IVR/classical Wigner model of thermal correlation functions[7] [and they called it the FK–LPI (linearized path integral) in Ref. 7].

Here we use the notation of the quantum correction factor $Q(u)$

$$Q\left(u=\beta\hbar\Omega\left(x_c\right)\right)=\frac{u/2}{\tanh\left(u/2\right)}, \tag{A1}$$

where the effective local frequency $\Omega(x_c)$ is obtained from the curvature of the Gaussian-averaged potential $V_s(x_c)$

$$m\Omega^2\left(x_c\right)=\left.\frac{\partial^2}{\partial x_c^2}\right|_{\theta^2(x_c)} V_s\left(x_c\right), \tag{A2}$$

$$V_s\left(x_c\right)=\int dy\,\left(\frac{\beta m\theta^2\left(x_c\right)}{2\pi}\right)^{1/2} \times\exp\left[-\beta\frac{1}{2}m\theta^2\left(x_c\right)\left(y-x_c\right)^2\right]V\left(y\right). \tag{A3}$$

$V_s(x_c)$ can be viewed as the classical thermal average of the potential function $V(y)$ for the Feynman–Kleinert (FK) harmonic oscillator whose equilibrium position is the centroid of the path in imaginary time [$x_c=\frac{1}{\beta\hbar}\int_0^{\beta\hbar}d\tau x(\tau)$] and whose frequency is given by

$$\theta^2\left(x_c\right)=\frac{\Omega^2\left(x_c\right)}{\frac{u/2}{\tanh\left(u/2\right)}-1}. \tag{A4}$$

Equations (A2) and (A4) need to be solved iteratively to obtain $\Omega(x_c)$ and $\theta(x_c)$.

Defining the effective (centroid) potential as

$$V_{\rm eff}\left(x_c\right)=V_S\left(x_c\right)-\frac{1}{2\beta}\left(\frac{u/2}{\tanh\left(u/2\right)}-1\right)+\frac{1}{\beta}\ln\left[\frac{\sinh\left(u/2\right)}{u/2}\right], \tag{A5}$$

the partition function is given by the FKA as[95,96]

$$Z=\int dx_c\left(\frac{m}{2\pi\hbar^2\beta}\right)^{1/2}\exp\left[-\beta V_{\rm eff}\left(x_c\right)\right]. \tag{A6}$$

Off-diagonal elements of the Boltzmann operator can also be approximated by the FKA as[96]

$$\begin{aligned}\left\langle x-\frac{\Delta x}{2}\right|e^{-\beta\hat{H}}\left|x+\frac{\Delta x}{2}\right\rangle^{\rm FKA}&\simeq\int dx_c\left(\frac{m}{2\pi\hbar^2\beta}\right)^{1/2}\exp[-\beta V_{\rm eff}\left(x_c\right)]\\&\times\left(\frac{\beta m\theta^2(x_c)}{2\pi}\right)^{1/2}\exp\left[-\beta\frac{1}{2}m\theta^2(x_c)(x-x_c)^2\right]\\&\times\exp\left[-\frac{m\Omega(x_c)}{4\hbar}\coth(u/2)\Delta x^2\right],\end{aligned} \tag{A7}$$

the Fourier transform of which gives the following expression for the Wigner density distribution[7,96] [e.g., Eq. (23) in Paper I]:

$$\mathsf{P}_{\rm W}^{eq,\ {\rm FKA}}\left(x,\,p\right)=\int dx_c\;\rho_{\rm W}^{eq,\ {\rm FKA}}\left(x,\,p;x_c\right), \tag{A8}$$

with

$$\begin{aligned}&\rho_{\rm W}^{eq,\ {\rm FKA}}\left(x,\,p;x_c\right)\\&=\frac{1}{\left(2\pi\hbar\right)}\exp\left[-\beta V_{\rm eff}\left(x_c\right)\right]\left(\frac{\beta m\theta^2\left(x_c\right)}{2\pi\,Q\left(u\right)}\right)^{1/2}\\&\times\exp\left[-\beta\frac{1}{2}m\theta^2\left(x_c\right)\left(x-x_c\right)^2-\beta\frac{p^2}{2m}\frac{1}{Q\left(u\right)}\right].\end{aligned} \tag{A9}$$

The quantum correction factor reflects $Q(u)$ how the local momentum distribution deviates from the classical momentum distribution.

In the imaginary frequency regime, as shown by Feynman and Kleinert,[95] the FKA is able to keep the imaginary frequency and temperature in the regime

$$u_i\equiv\beta\hbar\left|\Omega\left(x_c\right)\right|<2\pi, \tag{A10}$$

so that, by virtue of analytic continuation, the frequency of the FK harmonic oscillator

$$\theta^2(x_c) = \frac{|\Omega(x_c)|^2}{1 - \frac{u_i/2}{\tan(u_i/2)}} \tag{A11}$$

and the effective (centroid) potential

$$V_{\text{eff}}(x_c) = V_S(x_c) - \frac{1}{2\beta}\left(\frac{u_i/2}{\tan(u_i/2)} - 1\right) + \frac{1}{\beta}\ln\left[\frac{\sin(u_i/2)}{u_i/2}\right] \tag{A12}$$

are always well-defined. However, when the imaginary frequency and temperature are such that

$$u_i \equiv \beta\hbar|\Omega(x_c)| \geq \pi, \tag{A13}$$

(i.e., large enough imaginary frequency and/or low enough temperature), the quantum correction factor $Q(u)$ becomes negative. The LGA based on the FKA (LGA–FKA) leads to Eq. (A8) (the Wigner density distribution) with the quantum correction factor $Q(u)$ (for the local momentum distribution) given by

$$Q\left(u = \beta\hbar\Omega(x_c)\right) = \begin{cases} \dfrac{u/2}{\tanh(u/2)} & for\ real\ u \\ = \dfrac{1}{Q(u_i)} = \dfrac{\tanh(u_i/2)}{u_i/2} & for\ imaginary\ u = iu_i \end{cases}. \tag{A14}$$

(Since the FK harmonic oscillator frequency $\theta(x_c)$ and the effective potential $V_{\text{eff}}(x_c)$ are always well-defined for imaginary frequencies $u_i \in (0,\ 2\pi)$ [see Eqs. (A11) and (A12)], no modification is needed in the LGA–FKA.)[54]

By virtue of Eq. (46) in Paper I and Eq. (A8), the ELD effective force in the Wigner phase space satisfies

$$\int dx_c \rho_{\text{W}}^{eq,\text{FKA}}(x, p; x_c)\left(-\beta\frac{p}{m}\frac{1}{Q(u(x_c))}\right)\frac{\partial}{\partial x}V_{\text{eff}}^{\text{W-ELD}}(x, p) = \int dx_c \rho_{\text{W}}^{eq,\ \text{FKA}}(x, p; x_c)\frac{p}{m}\left[-\beta m\theta^2(x_c)(x - x_c)\right]. \tag{A15}$$

Since the above equation holds for any phase point $(x,\ p)$, we then have the expression of the ELD effective force

$$-\frac{\partial}{\partial x}V_{\text{eff}}^{\text{W-ELD}}(x, p) = -\left\{\int dx_c\ \rho_{\text{W}}^{eq,\ \text{FKA}}(x, p; x_c)\, Q(u(x_c))^{-1}\right\}^{-1} \times \int dx_c\ \rho_{\text{W}}^{eq,\ \text{FKA}}(x, p; x_c)\left[m\theta^2(x_c)(x - x_c)\right]. \tag{A16}$$

One can show the function f_{A^β} takes the form

$$\text{Re}\left[f_{A^\beta}^{\text{W}}(x, p)\right] = \frac{\int dx_c\ \rho_{\text{W}}^{eq,\ \text{FKA}}(x, p; x_c)\left[x^2 + \frac{\beta\hbar^2}{4mQ(u(x_c))} - \left(\frac{\beta\hbar p}{2mQ(u(x_c))}\right)^2\right]}{\int dx_c\ \rho_{\text{W}}^{eq,\ \text{FKA}}(x, p; x_c)}, \tag{A17}$$

for $\hat{A}^\beta = e^{-\beta\hat{H}}\hat{x}^2$; and

$$f_{A^\beta}^{\text{W}}(x, p) = \frac{\int dx_c\ \rho_{\text{W}}^{eq,\ \text{FKA}}(x, p; x_c)\left[\frac{p}{Q(u(x_c))}\right]}{\int dx_c\ \rho_{\text{W}}^{eq,\ \text{FKA}}(x, p; x_c)}, \tag{A18}$$

for $\hat{A}^\beta = \hat{p}_{\text{Kubo}}^\beta$.

The W-ELD correlations functions based on FKA for $\langle p(0)\, p(t)\rangle_{\text{Kubo}}$ and $\langle x^2(0)\, x^2(t)\rangle_{\text{std}}$ at the low temperature ($\beta = 8$) are shown in Figs. 8 and 9 for the two anharmonic models. (Results at the high temperature ($\beta = 0.1$) are the same as the W-ELD results in Figs. 2 and 5, not shown though.) The W-ELD with FKA behaves nearly the same as W-ELD with full TGA showing only slightly more dephasing in amplitude of the oscillation.

It is straightforward to derive equations for H-ELD with FKA along similar lines.

2. Thermal Gaussian approximations in the coherent state representation

There are several other thermal Gaussian approximations based on either the thawed or frozen Gaussian in coherent state, which are useful to accomplish the task for obtaining the Wigner or Husimi density distribution function. Particularly, similar to LGA–TGA [i.e., Eq. (43) for the Wigner density distribution function], it is possible to obtain the Husimi density distribution function $\langle x,\ p|\, e^{-\beta\hat{H}}\,|x,\ p\rangle$ at each phase point with only one imaginary-time trajectory by propagating the coherent state in imaginary time, as we propose below.

1. *Thermal frozen Gaussian*

One way is to propagate the frozen Gaussian[32] in imaginary time, as suggested by Zhang *et al.*[97]

$$\langle q|\exp\left(-\tau\hat{H}\right)|x,\ p\rangle \approx f(x, p; \tau)\langle q\ |x,\ p; \tau\rangle, \tag{A19}$$

where the frozen Gaussian is given by

$$\langle q\ |x,\ p;\tau\rangle = \frac{|\det(\Gamma)|^{1/4}}{\pi^{N/4}} \exp\left[-\frac{1}{2}(q - x(\tau))^T \Gamma (q - x(\tau)) + \frac{i}{\hbar} p(\tau)^T (q - x(\tau))\right], \tag{A20}$$

with

$$f(\tau) = \exp\left(-\int_0^\tau d\tau' \left[\frac{1}{2} p(\tau')^T M^{-1} p(\tau') + \langle V(x(\tau'))\rangle_{\mathrm{TFG}} + \frac{\hbar^2}{4}\mathrm{Tr}\left[\Gamma \mathrm{M}^{-1}\right] - \frac{i}{\hbar} p(\tau)^T \frac{\partial x(\tau')}{\partial \tau'}\right]\right), \tag{A21}$$

and the following equations of motion:

$$\frac{\partial x(\tau)}{\partial \tau} = -\Gamma^{-1} \langle \nabla V(x(\tau))\rangle_{\mathrm{TFG}}, \tag{A22}$$

$$\frac{\partial p(\tau)}{\partial \tau} = -\hbar^2 \Gamma \mathrm{M}^{-1} p(\tau), \tag{A23}$$

or, equivalently,

$$p(\tau) = \exp\left(-\hbar^2 \Gamma \mathrm{M}^{-1}\tau\right) p(0). \tag{A24}$$

The initial conditions for the imaginary-time propagation are

$$x(\tau = 0) = x; \quad p(\tau = 0) = p. \tag{A25}$$

The frozen Gaussian averages are defined as

$$\langle h(x(\tau))\rangle_{\mathrm{TFG}} = \left(\frac{1}{\pi}\right)^{N/2} |\det(\Gamma)|^{1/2} \int_{-\infty}^{\infty} dq \exp\left[-(q - x(\tau))^T \Gamma (q - x(\tau))\right] h(q). \tag{A26}$$

One can then get

$$\langle x,\ p|\, e^{-\beta\hat{H}}\, |x,\ p\rangle = \int dq\, \langle x,\ p|\, e^{-\beta\hat{H}/2}\, |q\rangle\, \langle q|\, e^{-\beta\hat{H}/2}\, |x,\ p\rangle = \exp\left\{-2W^{\mathrm{TFG}}\left(\frac{\beta}{2}; x,\ p\right)\right\}, \tag{A27}$$

with

$$\mathrm{W}^{\mathrm{TFG}}\left(\frac{\beta}{2}; x,\ p\right) = \frac{\beta\hbar^2}{8}\mathrm{Tr}\left[\Gamma M^{-1}\right] + \frac{1}{2} p^T \left(2\hbar^2\Gamma\right)^{-1} \times \left[\mathrm{I} - \exp\left(-\beta\hbar^2\Gamma\mathrm{M}^{-1}\right)\right] p + \int_0^{\beta/2} d\tau' \left[\langle V(x(\tau\prime))\rangle_{\mathrm{TFG}}\right]. \tag{A28}$$

Here I is the identity matrix. The expression for the partition function Z becomes

$$Z = \int dx \int dp\ \mathsf{P}_H^{eq,\mathrm{TFG}}(x,\ p) = \left(\frac{1}{2\pi\hbar}\right)^N \int dx \int dp\ \exp\left\{-2W^{\mathrm{TFG}}\left(\frac{\beta}{2}; x,\ p\right)\right\} \tag{A29}$$

as follows from Eq. (A27).

The ELD effective force is

$$-\frac{\partial}{\partial x} V_{\mathrm{eff}}^{\mathrm{H\text{-}ELD}}(x,\ p) = -2\hbar^2 \left[\mathrm{I} - \exp\left(-\beta\hbar^2\Gamma M^{-1}\right)\right]^{-1} \Gamma M^{-1} \times \int_0^{\beta/2} d\tau' \left[\partial \left\langle V(x(\tau'))\right\rangle_{\mathrm{TFG}} / \partial x\right]. \tag{A30}$$

One can show the function f_{A^β} takes the form

$$\begin{aligned}\mathrm{Re}\left[f_{A^\beta}^{\mathrm{W}}(x,\ p)\right] &= x^2 + (2\Gamma)^{-1} \\ &-2x\left\{\int_0^{\beta/2} d\tau \exp\left[-\hbar^2\Gamma M^{-1}\tau\right] \Gamma^{-1} \langle \nabla V(x(\tau; x))\rangle_{\mathrm{TFG}}\right\} \\ &+\left\{\int_0^{\beta/2} d\tau \exp\left[-\hbar^2\Gamma M^{-1}\tau\right] \Gamma^{-1} \langle \nabla V(x(\tau; x))\rangle_{\mathrm{TFG}}\right\}^2, \\ &-\left\{\left(2\hbar\Gamma\right)^{-1}\left(1 - \exp\left[-\hbar^2\Gamma M^{-1}\beta\right]\right) p\right\}^2\end{aligned} \tag{A31}$$

for $\hat{A}^\beta = e^{-\beta\hat{H}}\hat{x}^2$; and

$$f_{A^\beta}^{\mathrm{W}}(x,\ p) = M\left(\beta\hbar^2\Gamma\right)^{-1}\left[1 - \exp\left(-\hbar^2\Gamma M^{-1}\beta\right)\right] p, \tag{A32}$$

for $\hat{A}^\beta = \hat{p}_{\mathrm{Kubo}}^\beta$.

The H-ELD correlation functions based on TFG for $\langle p(0)p(t)\rangle_{\mathrm{Kubo}}$ and $\left\langle x^2(0)\, x^2(t)\right\rangle_{\mathrm{std}}$ at the low temperature ($\beta = 8$) are shown in Figs. 10 and 11 for the two anharmonic models. [The width parameter is chosen in the optimum regime, which depends on the correlation function and the TFG approximation. For instance, the optimum widths lie around $\Gamma = 1.63$ for $\langle p(0)\, p(t)\rangle_{\mathrm{Kubo}}$ and around$\Gamma = 1.72$ for $\left\langle x^2(0)\, x^2(t)\right\rangle_{\mathrm{std}}$ for the asymmetric anharmonic model (Eq. (57)); around $\Gamma = 1.32$ and around $\Gamma = 1.62$ respectively for the quartic potential (Eq. (58)).] Similar to W-ELD with LGA–TGA in which also only a single imaginary trajectory is involved at each phase point, H-ELD with TFG gives correlation functions that show dephasing in amplitude of the oscillation but still show systematical improvement over LSC–IVR. Comparison of Fig. 10 to Fig. 4 for the asymmetric anharmonic model and that of Fig. 11 to Fig. 7 for the purely quartic potential demonstrate that H-ELD with

TFG does not work as well as H-ELD with full TGA. TFG is the simplest but least accurate way to obtain the Husimi distribution function $\langle x,\, p|\, e^{-\beta\hat{H}}\,|x,\, p\rangle$ at each phase point $(x,\, p)$ for multidimensional condensed phase systems.

2. Thermal thawed Gaussian

Another approach is to follow Baranger *et al.*[41] with the thawed Gaussian propagated in imaginary time, as suggested by Pollak and Martin–Fierro[98]

$$\langle q|\exp\left(-\tau\hat{H}\right)|x,\, p\rangle \approx f\,(x,\, p;\tau)\,\langle q\;|x,\, p;\tau\rangle\,, \tag{A33}$$

where

$$\begin{aligned}\langle q\;|x,\, p;\tau\rangle = {}& \frac{|\det\Gamma\,(\tau)|^{1/4}}{\pi^{N/4}}\\ &\times\;\exp\left[-\frac{1}{2}\,(q-x\,(\tau))^{T}\,\Gamma\,(\tau)\,(q-x\,(\tau))\right.\\ &\left.+\;\frac{i}{\hbar}\,p\,(\tau)^{T}\,(q-x\,(\tau))\right],\end{aligned} \tag{A34}$$

and

$$\begin{aligned}f\,(\tau) = \exp\Bigg(-\int_0^{\tau} d\tau'\Bigg[&\frac{1}{2}\,p\,(\tau')^{T}\,M^{-1}\,p\,(\tau')+\left\langle V\left(x\,(\tau')\right)\right\rangle_{\mathrm{TTG}}\\ &+\frac{\hbar^2}{4}\mathrm{Tr}\left[\Gamma\,(\tau')\,M^{-1}\right]-\frac{i}{\hbar}\,p\,(\tau')^{T}\,\frac{\partial x\,(\tau\prime)}{\partial\tau'}\Bigg]\Bigg),\end{aligned} \tag{A35}$$

with the following equations of motion

$$\begin{aligned}\frac{\partial p\,(\tau)}{\partial\tau} &= -\hbar^2\Gamma\,(\tau)\,M^{-1}\,p\,(\tau)\,,\\ \frac{\partial x\,(\tau)}{\partial\tau} &= -\Gamma\,(\tau)^{-1}\,\langle\nabla V\,(x\,(\tau))\rangle_{\mathrm{TTG}}\,,\\ \frac{\partial\Gamma\,(\tau)}{\partial\tau} &= -\hbar^2\Gamma\,(\tau)\,M^{-1}\Gamma\,(\tau)+\left\langle\nabla\nabla^{T}\,V\,(x\,(\tau))\right\rangle_{\mathrm{TTG}}\,,\end{aligned} \tag{A36}$$

and the thawed Gaussian averages defined as

$$\begin{aligned}\langle h\,(x\,(\tau))\rangle_{\mathrm{TTG}} = {}& \left(\frac{1}{\pi}\right)^{N/2}|\det\left(\Gamma\,(\tau)\right)|^{1/2}\int_{-\infty}^{\infty}dq\\ &\times\exp\left[-\,(q-x\,(\tau))^{T}\,\Gamma\,(\tau)\,(q-x\,(\tau))\right]h\,(q)\,.\end{aligned} \tag{A37}$$

The initial conditions for the imaginary time propagation are

$$x\,(\tau=0)=x;\quad p\,(\tau=0)=p;\quad \Gamma\,(\tau=0)=\Gamma. \tag{A38}$$

One can then get

$$\begin{aligned}\langle x,\, p|\, e^{-\beta\hat{H}}\,|x,\, p\rangle &= \int dq\,\langle x,\, p|\, e^{-\beta\hat{H}/2}\,|q\rangle\,\langle q|\, e^{-\beta\hat{H}/2}\,|x,\, p\rangle\\ &= \exp\left(-2\mathrm{W}^{\mathrm{TTG}}\left(\tfrac{\beta}{2}\right)\right),\end{aligned} \tag{A39}$$

with

$$\begin{aligned}\mathrm{W}^{\mathrm{TTG}}\left(\frac{\beta}{2}\right) &= \int_0^{\beta/2} d\tau'\left[\frac{1}{2}p(\tau')^{T}M^{-1}p(\tau')+\left\langle V\left(x\left(\tau'\right)\right)\right\rangle_{\mathrm{TTG}}+\frac{\hbar^2}{4}\mathrm{Tr}[\Gamma\left(\tau'\right)M^{-1}]\right]\\ &= \frac{1}{2}p^{T}M^{-1}_{\mathrm{TTG}}\left(\frac{\beta}{2}\right)p+\int_0^{\beta/2} d\tau'\left[\left\langle V\left(x\left(\tau'\right)\right)\right\rangle_{\mathrm{TTG}}+\frac{\hbar^2}{4}\mathrm{Tr}[\Gamma\left(\tau'\right)M^{-1}]\right],\end{aligned} \tag{A40}$$

where

$$\begin{aligned}M^{-1}_{\mathrm{TTG}}\left(\frac{\beta}{2}\right) = {}& \int_0^{\beta/2} d\tau'\exp\left[-\hbar^2\int_0^{\tau'}\Gamma\,(\tau)\,d\tau\;M^{-1}\right]M^{-1}\\ &\times\;\exp\left[-\hbar^2\int_0^{\tau'}\Gamma\,(\tau)\,d\tau\;M^{-1}\right].\end{aligned} \tag{A41}$$

The expression for a partition function Z becomes

$$\begin{aligned}Z &= \int dx\int dp\;\mathsf{P}_{H}^{eq,\mathrm{TTG}}\,(x,\, p)\\ &= \left(\frac{1}{2\pi\hbar}\right)^{N}\int dx\int dp\;\exp\left\{-2\mathrm{W}^{\mathrm{TTG}}\left(\frac{\beta}{2};x,\, p\right)\right\},\end{aligned} \tag{A42}$$

based on Eq. (A39). TTG is expected to be more accurate and a little more expensive than TFG when only one imaginary trajectory is used to evaluate the Husimi distribution function $\langle x,\, p|\, e^{-\beta\hat{H}}\,|x,\, p\rangle$.

The ELD effective force becomes

$$\begin{aligned}-\frac{\partial}{\partial x}V^{\text{H-ELD}}_{\mathrm{eff}}\,(x,\, p) = {}& -M_{\mathrm{TTG}}\left(\frac{\beta}{2}\right)M^{-1}\int_0^{\beta/2}d\tau'\\ &\times\left[\left\langle\frac{\partial}{\partial x}V\left(x\left(\tau'\right)\right)\right\rangle_{\mathrm{TTG}}\right.\\ &\left.+\;\frac{\hbar^2}{4}\frac{\partial}{\partial x}\mathrm{Tr}\left[\Gamma\left(\tau'\right)M^{-1}\right]\right].\end{aligned} \tag{A43}$$

For either the thermal frozen Gaussian or thermal thawed Gaussian , in addition to our modified versions with only a single imaginary trajectory, one can also express the Boltzmann operator as

$$e^{-\beta\hat{H}} = \int dx'\int dp'\exp\left(-2\mathrm{W}\left(\frac{\beta}{2}\right)\right)\left|x',\, p';\frac{\beta}{2}\right\rangle\left\langle x',\, p';\frac{\beta}{2}\right|, \tag{A44}$$

as the original authors[97,98] did. One can then obtain the Wigner or Husimi density distribution in a similar way from

Eq. (35) or (48) [which is often more accurate but less efficient than Eq. (A27) or (A39)].

Note that all these approximations (in Sec. IV and the Appendix) for the Boltzmann operator are exact in the harmonic limit. Although we show most equations for one-dimensional cases in the paper, the generalization to multi-dimensional systems is straightforward.

We note two important points here. First, FKA (or LGA–FKA) and all TGAs (VGW, TFG, or TTG) require that the potential surface be accurately fitted by polynomials, exponentials, or Gaussians such that the Gaussian integrals [Eqs. (31), (A26) or (A39)] necessary to evaluate in the equations of motions could be evaluated analytically, otherwise performing these Gaussian integrals in multidimensional systems would be too computationally demanding. In this sense, FKA (or LGA–FKA) and all TGAs are not a good option for complex/large polyatomic molecular systems where angle and dihedral interactions (or dipole-induced dipole interactions) are important. Second, all TGAs suffer when imaginary frequencies become important as we first mentioned in our earlier paper[22] (e.g., chemical reactions and low-temperature molecular liquids[54]). An approach[87,97,98] has been proposed to consistently improve accuracies of all these TGAs, however, the approach meanwhile loses the merit of the TGAs—the Wigner or Husimi density distribution function could be obtained analytically without phase cancelling problems. The path integral representation of LGA[54] can overcome these problems. An efficient path integral representation of ELD will be discussed in a subsequent paper.

[1] B. J. Berne and G. D. Harp, Adv. Chem. Phys. **17**, 63 (1970).
[2] W. H. Miller, S. D. Schwartz, and J. W. Tromp, J. Chem. Phys. **79**, 4889 (1983).
[3] R. Kubo, M. Toda, and N. Hashitsume, *Statistical Physics II: Nonequilibrium Statistical Mechanics*, 2nd ed. (Springer-Verlag, Heidelberg, 1991).
[4] H. Wang, X. Sun, and W. H. Miller, J. Chem. Phys. **108**, 9726 (1998).
[5] X. Sun, H. Wang, and W. H. Miller, J. Chem. Phys. **109**, 7064 (1998).
[6] J. Liu and W. H. Miller, J. Chem. Phys. **126**, 234110 (2007).
[7] J. A. Poulsen, G. Nyman, and P. J. Rossky, J. Chem. Phys. **119**, 12179 (2003).
[8] Q. Shi and E. Geva, J. Chem. Phys. **118**, 8173 (2003).
[9] R. Hernandez and G. A. Voth, Chem. Phys. **233**, 243 (1998).
[10] E. Pollak and J. L. Liao, J. Chem. Phys. **108**, 2733 (1998).
[11] J. Shao and N. Makri, J. Phys. Chem. A **103**, 7753 (1999).
[12] J. Shao and N. Makri, J. Phys. Chem. A **103**, 9479 (1999).
[13] N. Makri, J. Phys. Chem. B **106**, 8390 (2002).
[14] N. J. Wright and N. Makri, J. Chem. Phys. **119**, 1634 (2003).
[15] A. Nakayama and N. Makri, J. Chem. Phys. **119**, 8592 (2003).
[16] N. J. Wright and N. Makri, J. Phys. Chem. B **108**, 6816 (2004).
[17] A. Nakayama and N. Makri, Chem. Phys. **304**, 147 (2004).
[18] N. Makri, A. Nakayama, and N. Wright, J. Theor. Comput. Chem. **3**, 391 (2004).
[19] A. Nakayama and N. Makri, Proc. Natl. Acad Sci. U.S.A. **102**, 4230 (2005).
[20] J. Liu and N. Makri, Chem. Phys. **322**, 23 (2006).
[21] J. Liu, A. Nakayama, and N. Makri, Mol. Phys. **104**, 1267 (2006).
[22] J. Liu and W. H. Miller, J. Chem. Phys. **125**, 224104 (2006).
[23] J. Kegerreis and N. Makri, J. Comput. Chem. **28**, 818 (2007).
[24] E. Bukhman and N. Makri, J. Phys. Chem. A **111**, 11320 (2007).
[25] J. Chen and N. Makri, Mol. Phys. **106**, 443 (2008).
[26] J. Kegerreis, A. Nakayama, and N. Makri, J. Chem. Phys. **128**, 184509 (2008).
[27] E. Bukhman and N. Makri, J. Phys. Chem. A **113**, 7183 (2009).
[28] W. H. Miller, J. Chem. Phys. **53**, 3578 (1970).
[29] W. H. Miller, J. Chem. Phys. **61**, 1823 (1974).
[30] W. H. Miller, Adv. Chem. Phys. **30**, 77 (1975).
[31] E. J. Heller, J. Chem. Phys. **62**, 1544 (1975).
[32] E. J. Heller, J. Chem. Phys. **75**, 2923 (1981).
[33] M. F. Herman and E. Kluk, Chem. Phys. **91**, 27 (1984).
[34] E. J. Heller, J. Chem. Phys. **95**, 9431 (1991).
[35] W. H. Miller, J. Chem. Phys. **95**, 9428 (1991).
[36] E. J. Heller, J. Chem. Phys. **94**, 2723 (1991).
[37] G. Campolieti and P. Brumer, Phys. Rev. A **50**, 997 (1994).
[38] K. G. Kay, J. Chem. Phys. **100**, 4377 (1994).
[39] K. G. Kay, J. Chem. Phys. **100**, 4432 (1994).
[40] D. J. Tannor and S. Garashchuk, Annu. Rev. Phys. Chem. **51**, 553 (2000).
[41] M. Baranger, M. A. M. de Aguiar, F. Keck, H. J. Korsch, and B. Schellhaass, J. Phys. A **34**, 7227 (2001).
[42] W. H. Miller, J. Phys. Chem. A **105**, 2942 (2001).
[43] K. G. Kay, Annu. Rev. Phys. Chem. **56**, 255 (2005).
[44] W. H. Miller, J. Chem. Phys. **125**, 132305 (2006).
[45] E. Pollak and J. S. Shao, J. Chem. Phys. **116**, 1748 (2002).
[46] T. Yamamoto, H. B. Wang, and W. H. Miller, J. Chem. Phys. **116**, 7335 (2002).
[47] J. Liu and W. H. Miller, J. Chem. Phys. **127**, 114506 (2007).
[48] J. Liu and W. H. Miller, J. Chem. Phys. **128**, 144511 (2008).
[49] J. Liu and W. H. Miller, J. Chem. Phys. **129**, 124111 (2008).
[50] Q. Shi and E. Geva, J. Phys. Chem. A **107**, 9070 (2003).
[51] B. J. Ka, Q. Shi, and E. Geva, J. Phys. Chem. A **109**, 5527 (2005).
[52] B. J. Ka and E. Geva, J. Phys. Chem. A **110**, 9555 (2006).
[53] I. Navrotskaya and E. Geva, J. Phys. Chem. A **111**, 460 (2007).
[54] J. Liu and W. H. Miller, J. Chem. Phys. **131**, 074113 (2009).
[55] J. Liu, W. H. Miller, F. Paesani, W. Zhang, and D. Case, J. Chem. Phys. **131**, 164509 (2009).
[56] J. A. Poulsen, G. Nyman, and P. J. Rossky, J. Phys. Chem. B **108**, 19799 (2004).
[57] J. A. Poulsen, G. Nyman, and P. J. Rossky, Proc. Natl. Acad. Sci. U.S.A. **102**, 6709 (2005).
[58] J. A. Poulsen, G. Nyman, and P. J. Rossky, J. Chem. Theory Comput. **2**, 1482 (2006).
[59] J. Cao and G. A. Voth, J. Chem. Phys. **99**, 10070 (1993).
[60] S. Jang and G. A. Voth, J. Chem. Phys. **111**, 2371 (1999).
[61] T. D. Hone, P. J. Rossky, and G. A. Voth, J. Chem. Phys. **124**, 154103 (2006).
[62] I. R. Craig and D. E. Manolopoulos, J. Chem. Phys. **121**, 3368 (2004).
[63] T. F. Miller and D. E. Manolopoulos, J. Chem. Phys. **123**, 154504 (2005).
[64] B. J. Braams and D. E. Manolopoulos, J. Chem. Phys. **125**, 124105 (2006).
[65] Q. Shi and E. Geva, J. Chem. Phys. **119**, 9030 (2003).
[66] A. Horikoshi and K. Kinugawa, J. Chem. Phys. **122**, 174104 (2005).
[67] A. Witt, S. D. Ivanov, M. Shiga, H. Forbert, and D. Marx, J. Chem. Phys. **130**, 194510 (2009).
[68] E. Wigner, Phys. Rev. **40**, 749 (1932).
[69] E. P. Wigner, *Perspectives in Quantum Theory* (MIT, Cambridge, 1971).
[70] K. Husimi, Proc. Phys. Math. Soc. Japn **22**, 264 (1940).
[71] R. J. Glauber, Phys. Rev. **131**, 2766 (1963).
[72] R. J. Glauber, *Quantum Optics and Electronics* (Gordon and Breach, New York, 1965).
[73] E. C. G. Sudarshan, Phys. Rev. Lett. **10**, 277 (1963).
[74] J. G. Kirkwood, Phys. Rev. **44**, 31 (1933).
[75] A. W. Rihaczek, IEEE Trans. Inf. Theory **14**, 369 (1968).
[76] C. L. Mehta, J. Math. Phys. **5**, 677 (1964).
[77] D. C. Rivier, Phys. Rev. **83**, 862 (1951).
[78] H. Margenau and R. N. Hill, Prog. Theor. Phys. **26**, 722 (1961).
[79] M. Born and P. Jordan, Z. Phys. **34**, 858 (1925).
[80] L. Cohen and Y. I. Zaparovanny, J. Math. Phys. **21**, 794 (1980).
[81] J. Kruger, in *Second International Wigner Symposium* (Goslar, Germany, 1991).
[82] P. D. Drummond and C. W. Gardiner, J. Phys. A **13**, 2353 (1980).
[83] L. Cohen, J. Math. Phys. **7**, 781 (1966).
[84] B. Hellsing, S. I. Sawada, and H. Metiu, Chem. Phys. Lett. **122**, 303 (1985).
[85] P. Frantsuzov, A. Neumaier, and V. A. Mandelshtam, Chem. Phys. Lett. **381**, 117 (2003).

[86]P. A. Frantsuzov and V. A. Mandelshtam, J. Chem. Phys. **121**, 9247 (2004).
[87]J. S. Shao and E. Pollak, J. Chem. Phys. **125**, 133502 (2006).
[88]E. Jezek and N. Makri, J. Phys. Chem. **105**, 2851 (2001).
[89]M. Thoss, H. Wang, and W. H. Miller, J. Chem. Phys. **114**, 9220 (2001).
[90]S. Zhang and E. Pollak, J. Chem. Phys. **121**, 3384 (2004).
[91]N. Makri and K. Thompson, Chem. Phys. Lett. **291**, 101 (1998).
[92]K. Thompson and N. Makri, J. Chem. Phys. **110**, 1343 (1999).
[93]D. M. Ceperley, Rev. Mod. Phys. **67**, 279 (1995).
[94]R. Giachetti and V. Tognetti, Phys. Rev. Lett. **55**, 912 (1985).
[95]R. P. Feynman and H. Kleinert, Phys. Rev. A **34**, 5080 (1986).
[96]A. Cuccoli, R. Giachetti, V. Tognetti, R. Vaia, and P. Verrucchi, J. Phys. Condens. Matter **7**, 7891 (1995).
[97]D. H. Zhang, J. S. Shao, and E. Pollak, J. Chem. Phys. **131**, 044116 (2009).
[98]E. Pollak and E. Martin-Fierro, J. Chem. Phys. **126**, 044116 (2007).